Journal of Volcanology and Geothermal Research 416 (2021) 107282

Contents lists available at ScienceDirect

Journal of Volcanology and Geothermal Research

journal homepage: www.elsevier.com/locate/jvolgeores

Modelling spatial population exposure and evacuation clearance time for the Auckland Volcanic Field, New Zealand

Alec J. Wild [a,*], Mark S. Bebbington [b], Jan M. Lindsay [a], Danielle H. Charlton [a]

[a] School of Environment, University of Auckland, Private Bag 92019, Auckland 1142, New Zealand
[b] Volcanic Risk Solutions, Massey University, Private Bag 11222, Palmerston North 4442, New Zealand

ARTICLE INFO

Article history:
Received 17 December 2020
Received in revised form 12 May 2021
Accepted 16 May 2021
Available online 19 May 2021

Keywords:
Emergency management
Volcanic Risk
Evacuation
Hazard
Auckland Volcanic Field

ABSTRACT

Auckland, New Zealand's largest city (population of ~1.6 million), is situated atop the monogenetic Auckland Volcanic Field (AVF). As in many places faced with volcanic activity, evacuation is seen as the best risk mitigation strategy for preserving lives in the event of volcanic unrest and/or an eruption. However, planning for an evacuation can be challenging. In particular, the uncertainty in vent location resulting from the monogenetic nature of the field makes identifying neighbourhoods to be evacuated impractical until well into the pre-eruption unrest period. This study uses spatial analysis methods to assess exposure for both population and private transport ownership as well as to identify those areas requiring public transport support for an evacuation. These data were overlaid on a range of possible vent locations across the AVF using a 500 × 500 m grid. At each possible vent location, a 5 km evacuation zone is modelled, following the official contingency plan for evacuation in a future AVF event. In order to simulate vent location uncertainty leading up to a future eruption, a range of buffer distances were applied around the modelled vent locations.

The exposure data derived were then used to model evacuation clearance time, which considered four phases: 1) the time taken to decide to call an evacuation; 2) the public notification time; 3) the evacuee's time to prepare; and 4) evacuee's travel time to beyond the evacuation zone. The length of time involved in phases 1 to 3 are all independent of the vent location; our analysis found these phases could be completed within 36 h, with over 80% confidence. Travel times to beyond the evacuation zone were modelled using the exposure analysis for population and private transport ownership combined with road network data and vehicle carrying capacity. This revealed travel times for this phase ranging from less than 1 up to 11 h, depending on traffic congestion, when considering no vent uncertainty. By combining the times modelled for all four phases, we found that when there is high certainty in the vent location, the median total evacuation clearance time with no congestion is approximately 37 h. However, include a 10 km vent uncertainty buffer into the model, the evacuation clearance time can increase to between 38 and 55 h, dependent on traffic congestion. A vent in the densely populated inner Auckland and CBD area would result in the greatest population required to evacuate, and also the greatest need for public transport support given the low vehicle ownership in this area. Our results can be used to inform emergency management decision making, and the model can be adapted for other regions as well as for other hazards.

1. Introduction

More than 10% of the world's population live within 100 km of an active volcano, posing a potentially significant risk and even fatal consequences to this group (Brown et al., 2015). With an increasing global population expanding into previously uninhabited volcanic regions, the number of people exposed is only likely to grow (Auker et al., 2013; Chester et al., 2000; Small and Naumann, 2001). At signs of volcanic unrest, evacuation is a common strategy used to mitigate risk to life, especially from proximal volcanic hazards such as ballistic ejecta and topographically controlled hazards such as pyroclastic flows and lahars (Marzocchi and Woo, 2007; Moriarty et al., 2007; Wilson et al., 2012). While improved volcanic monitoring, public awareness and communication have likely contributed to the decrease in the annualised rate of volcanic fatalities in the last few decades (Auker et al., 2013; Barclay et al., 2019; Brown et al., 2017), there is also a valuable

Abbreviations: AVF, Auckland Volcanic Field; CDEM, Civil Defence and Emergency Management; ECT, Evacuation Clearance Time; EMA, Emergency Management Alerts; GDP, Gross Domestic Product; NEMA, National Emergency Management Agency; NZVSAP, New Zealand Volcanic Science Advisory Panel; PEZ, Primary Evacuation Zone; SEZ, Secondary Evacuation Zone.

* Corresponding author.
E-mail address: awil302@aucklanduni.ac.nz (A.J. Wild).

https://doi.org/10.1016/j.jvolgeores.2021.107282

role for timely decision-making and clear and appropriate management and coordination to ensure that evacuations are as efficient as possible (Hong and Frias-Martinez, 2020).

Evacuations have been conducted during many past volcanic crises around the world, including the 1991 Mt. Pinatubo eruption (Newhall et al., 1998; Newhall and Punongbayan, 1996), the 1999 Tungurahua eruption (Lane et al., 2003; Tobin and Whiteford, 2002) and the 1976–1977 eruption of La Soufrière volcano in Guadeloupe (Chenet et al., 2014). The desire to reduce risk to life from volcanic activity, together with statutory requirements to mitigate natural hazard (including volcanic) risk around the world, have led to the development of evacuation and volcanic contingency plans (e.g. Auckland, New Zealand; Auckland Council, 2015), as well as emergency management planning and crisis response exercises (e.g. in Italy; Marzocchi et al., 2008, and in Iceland; Guðmundsson and Gylfason, 2005; Bird et al., 2009).

While often the optimal measure to save lives, the decision to call an evacuation is complex. A balance must be struck between life preservation and the harmful disruption and high political and economic costs associated with the risk of a "false alarm" (Woo, 2008). Decision makers must also navigate the fear of public backlash, loss of credibility and legal repercussions from an unrequired evacuation (Bretton et al., 2017, 2015; Dow and Cutter, 1998; Marzocchi, 2012; Marzocchi and Woo, 2007; Papale, 2017). A key piece of information to support decision-makers is understanding the population exposed to a given hazard, and the time required to evacuate to safety. Contingency plans are typically informed through analysis of population exposure. For example, it was identified that between 200,000 and 400,000 people would be at risk in Naples from a modest eruption of Campi Flegrei (Barberi and Carapezza, 1996). Such data can be incorporated into quantitative approaches to support decision-makers. Evacuation triggers or thresholds could be established through the use of cost-benefit analysis, which balances the cost of action versus the loss from no action (Bebbington and Zitikis, 2016; Marzocchi and Woo, 2009, 2007; Woo, 2008). Population exposure data and cost-benefit analysis can be combined with eruption forecasting models to provide quantitative input to support decision-makers in real-time (Marzocchi and Woo, 2007; Sandri et al., 2012; Wild et al., 2019b).

Auckland, located in New Zealand's North Island (Fig. 1a), is the country's largest city (population ~ 1.6 million; Statistics New Zealand, 2018) and is responsible for 37.9% (NZ$$_{2018}$$107.8 billion; Statistics New Zealand, 2019a) of the nation's GDP. Auckland is also situated upon the monogenetic Auckland Volcanic Field (AVF). The monogenetic nature of the AVF poses a significant challenge to forecasting the next eruption location. Previous studies have developed long-term spatial forecast models (Bebbington, 2015, 2013; Bebbington and Cronin, 2011), showing the spatial intensity for future vent locations in the AVF. Meanwhile it has been hypothesised that in the event of a future unrest period, the localisation of seismicity will be indicative of future vent opening (Lindsay et al., 2010; Sherburn et al., 2007). Estimates of AVF eruption warning time based on published proposed magma ascent rates (0.01–6 $m.s^{-1}$; Blake, 2006; Brenna et al., 2018; Kereszturi et al., 2014) vary from <2 h through to 35 days, assuming detection of seismicity from 25 to 30 km at the mantle-crust boundary (Horspool et al., 2006; Sherburn et al., 2007). However, waiting for the localisation of seismicity can cause delays in assessing the population exposure and subsequent evacuation clearance times. In addition, Auckland's geography creates logistical challenges for evacuation planning. Because of the isthmus on which Auckland is located, all land-based transport is restricted through narrow stretches (Fig. 1b). Although these narrow stretches include at least one state highway, they can still become congested with an influx of vehicles, as witnessed on a daily basis during peak-hour traffic (Auckland Transport, 2020). While mass evacuation will be required in the event of a future AVF eruption (Auckland Council, 2015), given the limited points of egress and bottlenecks on either side of the isthmus and the large population of Auckland, the process of planning for an evacuation is logistically challenging (Blake et al., 2017; Tomsen et al., 2014; Woo, 2008). Hence, to support decision-makers during a future eruption in Auckland, planning is required, with one vital step being the assessment of population exposure and subsequent evacuation clearance time for people within the yet to be defined evacuation zone.

This paper presents a spatial model of population exposure and evacuation clearance time for the Auckland Volcanic Field, New Zealand, using a combination of geospatial and statistical approaches. The remainder of the paper is structured as follows: First, we review the volcanic hazard and risk and current assessment of evacuation difficulty in Auckland. A geospatial exposure assessment for the AVF is then presented. This assessment is subsequently used to model the spatial-temporal distribution of evacuation clearance times to provide estimates for how long it would take people to clear a hypothetical evacuation zone in the event of a future AVF eruption.

2. The Auckland Volcanic Field

The Auckland Volcanic Field is a monogenetic field with an estimated 53 eruptive centres distributed across 360 km^2. It formed over the last ~190 ka, with the last eruption occurring 550–600 years ago (Allen and Smith, 1994; Hopkins et al., 2020; Leonard et al., 2017; Lindsay et al., 2011; Smid et al., 2009). Most of these eruptions have been <0.1 km^2 in volume, however, the most recent two eruptions, namely Mt. Wellington and Rangitoto, have been significantly larger than average (Kereszturi et al., 2013).

In the AVF, the majority of past eruptions have a phreatomagmatic phase (Ang et al., 2020; Kereszturi et al., 2014). Phreatomagmatic eruptions occur due the explosive interaction of magma with water, either seawater if in the ocean or groundwater if on land (Morrissey et al., 2000). Some AVF eruptions stop after this stage, leaving maar craters, whereas others can progress onto a Hawaiian magmatic phase, producing lava flows and scoria cones (Kereszturi et al., 2014). In the AVF, phreatomagmatic eruptions have produced dilute pyroclastic density currents (PDCs), often referred to as base-surges (Brand et al., 2014; Wohletz and Sheridan, 1979). Base-surges can travel at speeds of up to 200–300 km/ h and exceed 200 °C (Belousov et al., 2007). It is considered for an average sized AVF eruption (0.01–0.1 km^3; Kereszturi et al., 2013), a base-surge could extend 2–4 km from the vent (Brand et al., 2014), exemplified by the Pupuke eruption in the AVF (0.047 km^3; Kereszturi et al., 2013), where surge deposits were found 3 km from the vent (Allen et al., 1996). For a large eruption (> 0.1 km^3; Kereszturi et al., 2013), a base-surge could reach distances of up to 6 km (Brand et al., 2014; Hopkins et al., 2017; Sandri et al., 2012). The base-surge hazard is considered the most significant early hazard due to its deadly and destructive nature and potentially large number people exposed to its effects (Sandri et al., 2012).

The monogenetic nature of the AVF means that each eruption has typically occurred in a different location across the field (Fig. 1c). One of the key challenges is thus identifying the location of the next future eruptive vent. Previous studies have looked at the spatial distribution of the next vent location in the AVF using probabilistic approaches for both long-term assessments (Bebbington, 2015, 2013; Bebbington and Cronin, 2011; Magill et al., 2005) and short-term crisis response (Lindsay et al., 2010). In addition, scenarios have been developed to look specifically at the societal impact to Auckland, including the number of people affected, from a future AVF eruption (Auckland Region CDEM Group, 2008; Deligne et al., 2017, 2015; Hayes et al., 2019, 2018). Past work examining likely impacts to Auckland from a future AVF eruption indicates that evacuation is key to preserving life (Blake et al., 2017; Deligne et al., 2017; Lindsay et al., 2011; Magill and Blong, 2005; Sandri et al., 2012; Tomsen et al., 2014).

The Auckland Volcanic Field Contingency Plan (Auckland Council, 2015) stipulates that faced with the threat of a volcanic eruption in Auckland, an evacuation is needed if a "hazard assessment indicates an urban

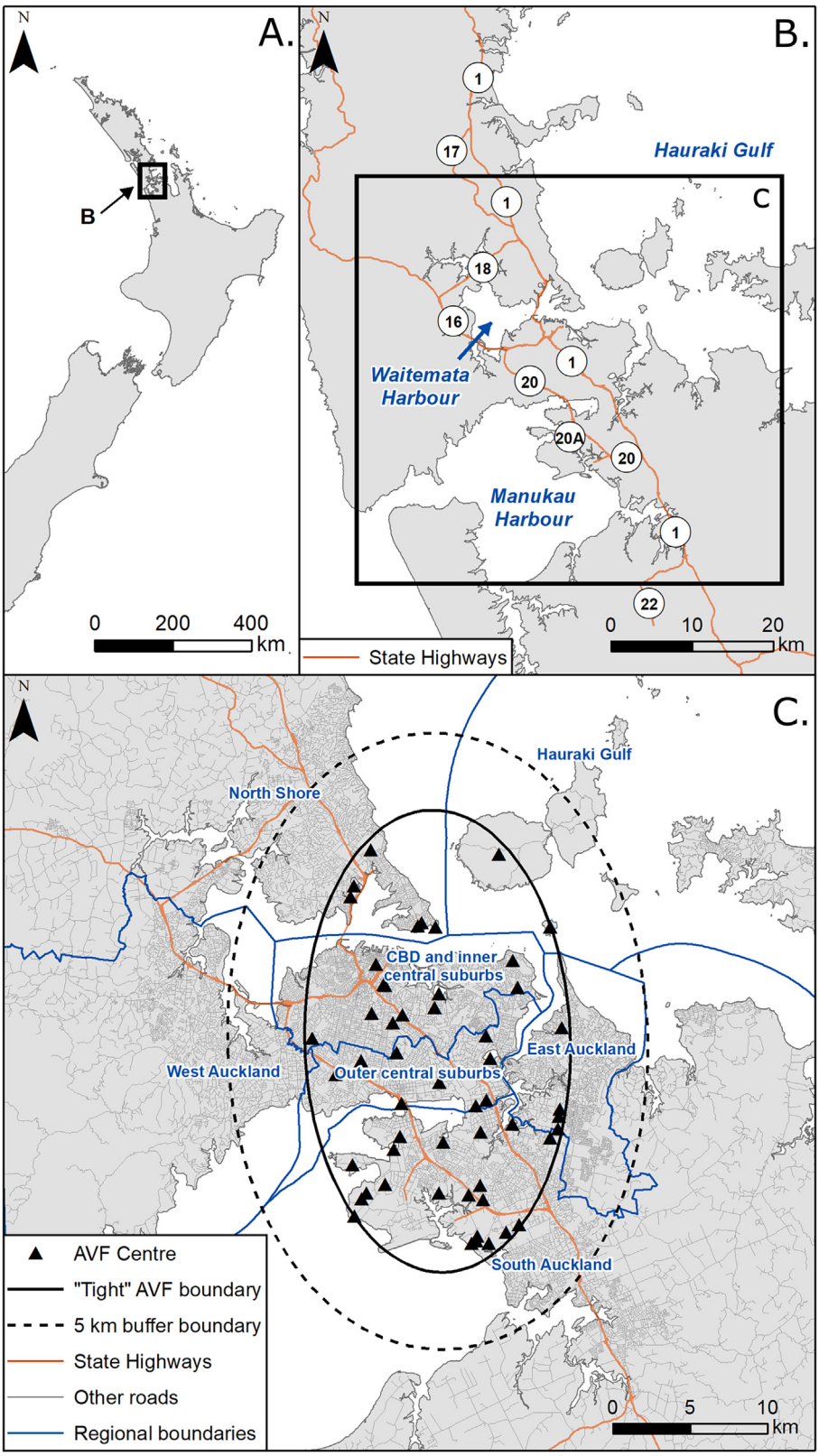

Fig. 1. (A) Location of Auckland in New Zealand's North Island, (B) Geography of Auckland's isthmus, state highways and harbours, and (C) Auckland Volcanic Field vent locations with "tight" and 5 km buffer boundary from Runge et al. (2015) to illustrate the current understanding of the AVF extent. The 5 km buffer is a conservative estimate of the maximum extent of the AVF. For the purposes of this study, Local Board areas (Statistics New Zealand, 2019b) were grouped to form seven distinct regions within Auckland.

or strategic area may lie within 5 km of the inferred eruption centre and/or there is potential risk to life". To prepare and support Auckland local authorities, the mass evacuation plan (Auckland Council, 2014) and Auckland Volcanic Field Contingency Plan (Auckland Council, 2015) were developed. The mass evacuation plan is designed to be hazard agnostic, and outlines the key considerations when making the decision to call an evacuation, such as the requirements around declaration of a state of emergency. Given the significance of Auckland nationally, considerations and requirements from national level agencies are also included. The decision to call an evacuation is made by the Auckland Emergency Management controller, but relies on input from various other groups such as the police and evacuation control team, logistics and welfare groups (Auckland Council, 2014). The New Zealand Volcano Science Advisory Panel (NZVSAP; including the former Auckland Volcanic Science Advisory Group) will provide scientific information relating to the state of the volcano as well as broader hazard and impact advice to the regional and national emergency management agencies to inform their decision-making (Auckland Council, 2015; Doyle et al., 2015). NZVSAP comprises expertise from both the legislated monitoring agency GNS Science/GeoNet as well as from universities and other agencies such as the New Zealand Metservice (NEMA, 2020).

The AVF Contingency Plan (Auckland Council, 2015) provides specific guidance and planning around evacuation orders in the event of a future volcanic event in Auckland. The plan establishes two evacuation zones: the primary evacuation zone (PEZ) and the secondary evacuation zone (SEZ). The PEZ corresponds to the high hazard zone and is defined as the area extending 3 km radially around the area considered the future vent location, the latter henceforth referred to as the vent uncertainty area. The SEZ extends a further 2 km radially from the PEZ and represents the moderate hazard zone. However, even with this differentiation, in a future crisis both the PEZ and SEZ are required to evacuate (Auckland Council, 2015; Deligne et al., 2017). Evacuations are likely to be conducted using a staged approach, with the PEZ given priority, especially when the vent uncertainty area remains large (Deligne et al., 2017; Wild et al., 2019a). The AVF Contingency Plan indicates evacuation of both the PEZ and SEZ should commence at moderate to heightened volcanic unrest, which aligns to level 2, the highest pre-eruption level in the current Volcanic Alert Level (VAL) system applied in New Zealand (Potter et al., 2014).

In 2008, a Civil Defence exercise called Exercise Rūaumoko was carried out in Auckland, in which the lead-up phase to an AVF eruption was simulated (Auckland Region CDEM Group, 2008; Brunsdon and Park, 2009; Horrocks, 2008). This exercise was designed to test New Zealand's nationwide arrangements for responding to a future volcanic eruption in Auckland, and included members from GNS Science, New Zealand's volcanic monitoring agency, and regional and national emergency management authorities. The "volcano" provided injects on precursory activity for scientists to interpret on a daily basis, which they used to prepare volcanic alert bulletins to provide to the emergency managers.

Blake et al. (2017) and Deligne et al. (2017) extended the Exercise Rūaumoko scenario to beyond the lead up phase, to review the wider built environment impacts and population displacement related to an actual eruption. In their scenario, an official evacuation was called seven days before the eruption, when the VAL increased from 1 to 2 in the original exercise (Deligne et al., 2017; Lindsay et al., 2010). The vent uncertainty area at this time remained large, represented as a 19×5 km northwest-southeast trending oblong shape stretching across the central isthmus, a region comprising of a mix of industry and residential land-use. A PEZ was formed by applying a ~ 1 km buffer around the vent uncertainty area, which would have required an evacuation of 199,200 people (Blake et al., 2017). Four days before the eruption, the area capturing the likely vent area had moved southwest and changed shape to include an oval centred over a predominantly residential area, increasing the number of people required to evacuate to 253,700. During the lead up to the eruption onset, the vent uncertainty decreased, but the evacuation zones increased with the addition of the full PEZ and SEZ as presented in the AVF Contingency Plan, which increased the number of people required to hypothetically evacuate to 362,100.

Tomsen et al. (2014) reviewed population exposure for a grid of hypothetical vents located across the AVF using 3.5, 5 and 8 km evacuation zone radii for both night- and day-time populations. The night-time population distribution was based on census data, derived based on primary residence. Day-time population data was developed using modelled assumptions from business and education datasets. The average night-time population exposure for the 3.5, 5 and 8 km evacuation zone radii was modelled as 27,210, 55,077 and 137,317, respectively. The maximum night-time population exposure was modelled as 131,841, 239,895 and 397,549 for the 3.5, 5 and 8 km evacuation zone radii, respectively. For the day-time exposure, the average was similar to the average at night-time, but the day-time maximums were significantly greater, due to the diurnal movement of people coming from the outer suburbs with lower population density into the CBD for work and education during the day.

Auckland's physical geography is such that potential evacuation routes are constrained along narrow corridors connecting parts of Auckland, which form the egress routes beyond a future AVF evacuation zone. Tomsen et al. (2014) looked at spatial evacuation planning in the AVF and population exposure at a neighbourhood level (boundaries defined by saltwater inlets, motorways, and major and arterial roads), accounting for both diurnal exposure, and the ease of evacuation (the latter based on an assessment of number of cars per household). They evaluated evacuation vulnerability by calculating population-, household- and car-to-exit capacity ratios, an approach first proposed by Cova and Church (1997). This approach expresses the evacuation demand per neighbourhood unit as the sum of the elements (e.g. population, households or number of vehicles) over the exit capacity, defined as the number of lanes intersecting the neighbourhood boundary. The largest shift in diurnal movement of evacuation demand was seen in the CBD, airport and industrial areas, where high evacuation demand during the day is not seen at night when workers return home, resulting in a shift in demand to residential suburbs at night.

Tomsen et al. (2014) modelled intra-regional evacuation travel times across Auckland and found these ranged from 1 to 9 h. However, Tomsen et al. (2014) did not consider the overall clearance time, which includes arriving at an evacuation call and notifying the public, but focused on the ease of evacuation with available egress and transport options and how long it would take to clear a defined region if people all departed at the same time. This is unrealistic, as an evacuation consists of a range of temporal factors, including the time-varying vent location uncertainty (Auckland Council, 2015; Lindsay et al., 2010; Sandri et al., 2012), the time to receive the evacuation order and individuals' preparation time prior to evacuating (Lindell, 2008; Lindell et al., 2020; Urbanik et al., 1980). Moreover, Tomsen et al. (2014) assess population exposure and evacuation clearance time independent of the spatial probability of vent location within the AVF, something this study explores using previous AVF spatial distribution models (Bebbington, 2013, 2015; Bebbington and Cronin, 2011).

3. Methods

Our methodological steps for conducting 1) the population exposure assessment and 2) the evacuation clearance time analysis are presented conceptually in Fig. 2. This outlines first the generic model inputs required for such an analysis, as well as the inputs relevant for our AVF application.

3.1. Population exposure analysis

We present a method for assessing the spatial variability in number of people within an evacuation zone across the AVF, considering both

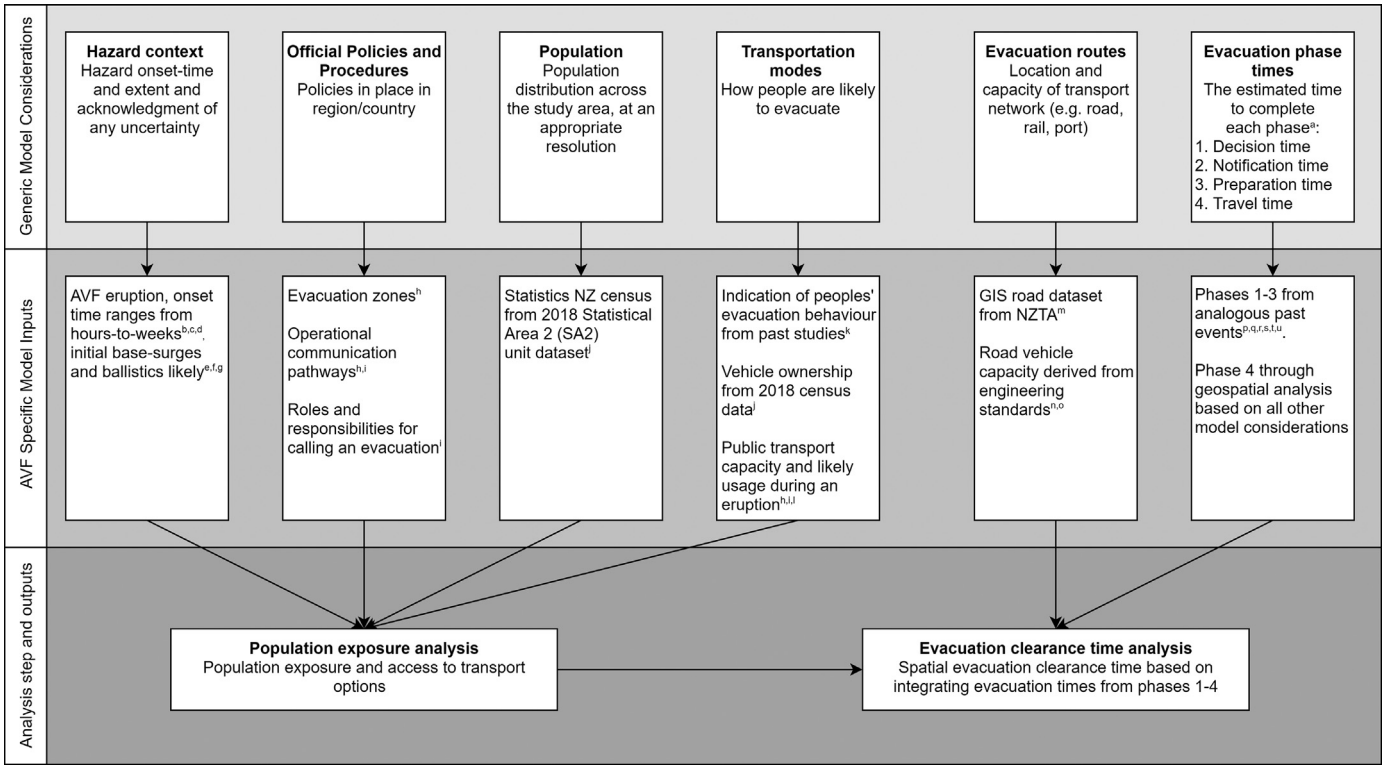

Fig. 2. Conceptual framework applied in this study demonstrating the generic input types for conducting such an assessment, as well as the inputs relevant for our AVF application. a Urbanik et al. (1980); b Blake (2006); c Brenna et al. (2018); d Kereszturi et al. (2014); e Brand et al. (2014); f Hopkins et al. (2020); g Sandri et al. (2012); h Auckland Council (2015); i Auckland Council (2014); j Statistics New Zealand (2018); k Coomer et al. (2015); l Auckland Transport (2020, pers. comm., 20 April 2020); m NZTA (Received 18 October 2019); n Green et al. (2020); p Cronin (2008); q Lindell (2008); r Lindell et al. (2020); s Perry (2007); t Trevett (2020); u Wu et al. (2012).

the PEZ and SEZ. Runge et al. (2015) identified an AVF boundary, but recommended using a buffer around this boundary to account for possible ongoing expansion of the field, due to either possible eruptions near the boundary (Lindsay et al., 2011) or anomalously large eruptions, such as Rangitoto, where the vent is within the current extent of the field, but the products extend beyond it (Kereszturi et al., 2013; Needham et al., 2011). Runge et al. (2015) suggested a 5 km buffer for the boundary, which, while likely conservative, is considered appropriate for this study. Here we approximate the spatial dimension of the AVF, including the 5 km buffer, as a series of 3312 evenly spaced 500 × 500 m grid points, defined as the possible vent locations, to represent the spatial uncertainty in a future eruption location.

The population data used in this study were retrieved from the 2018 census (Statistics New Zealand, 2018). The spatial data unit used is the Statistics New Zealand Statistical Area Two (SA2) (Fig. 3a). The SA2 size in the urban environment represents a "semi-suburb" resolution, and is the second smallest census data unit available. The SA2 unit was selected as it is the census data unit closest in size to the operational evacuation boundaries presented as part of the 2008 Exercise Rūaumoko (Auckland Region CDEM Group, 2008). SA1, the smallest census data unit, is the size of a residential block in densely populated areas. It is likely that this is too granular for crisis decisions, given that evacuation orders are typically provided on a suburb level, or by using the bounds of major roads or geographic features (e.g. coastlines) (e.g. Tomsen et al., 2014). The census data is a record of where the population resides, so a limitation is that it represents the night-time population distribution and does not consider diurnal movements, such as going to work or school. However, a survey of Aucklanders carried out after Exercise Rūaumoko suggested that most people (93.4%) would likely evacuate as a household (Coomer et al., 2015), which, irrespective of their daily movement, suggests families will return from school or work to their homes prior to evacuation. In this study, we assume evacuation will occur from primary residences only.

Data on number of households and vehicles owned by households were also derived from the census data. The total number of cars is required for this analysis, and the data on cars per household is used to derive this. The number of cars per census unit is calculated using Eq. 1, and follows the same approach as that presented by Tomsen et al. (2014) (Fig. 3b).

$$Cars = n_{hh}(1\ car) \times 1 + n_{hh}(2\ cars) \times 2 + n_{hh}(3\ cars) \times 3 + n_{hh}(4\ cars) \times 4 + n_{hh}(5\ or\ more\ cars) \times 5 \quad (1)$$

Where n_{hh} represents the number of households in each census unit with that many vehicles.

While this approach potentially underestimates the number of cars as it assumes no household has more than five cars, this relates to a small proportion (< 3% of households) of the population. More importantly, an estimate of the population without access to motor vehicles can be derived by multiplying the number of households without a privately-owned vehicle by the average occupancy per household for that census unit. This is vital as it identifies the number and location of those likely needing public transport support to evacuate. This identifies the CBD and the surrounding inner suburbs as the main areas in which households do not own a vehicle (Fig. 3c).

Spatial overlay analysis is applied to assess the population exposure across the AVF. At each hypothetical vent location across the grid, a radial area of 3 and 5 km, representing the PEZ and SEZ distance respectively, is generated. The sum of the population, number of vehicles and estimated population without a vehicle within the SA2 units that are either within or intersect the evacuation zone area is evaluated (Fig. 4). While this includes a proportion of the population not explicitly within the SEZ, it is deemed a more appropriate method for assessing the extent of population within an evacuation zone formed during a crisis, and aligns with procedures during emergency management exercises (Blake et al., 2017).

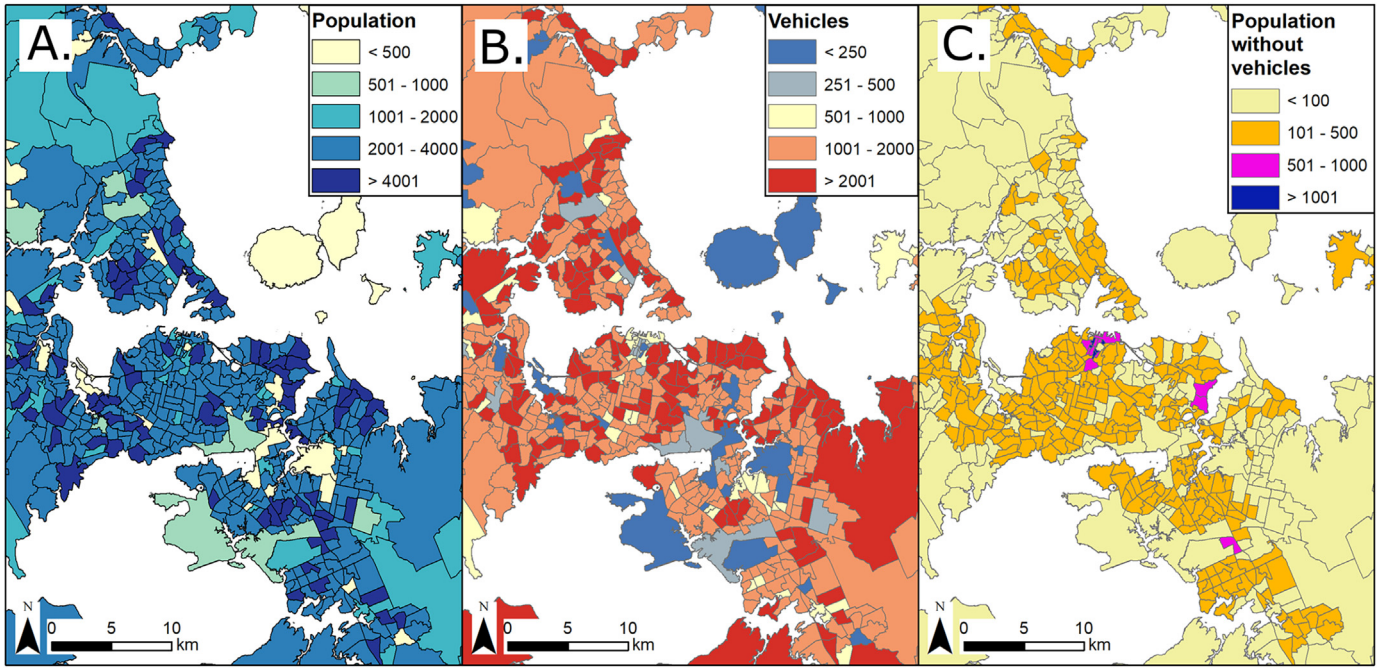

Fig. 3. Distribution of (A) population, (B) number of vehicles (C) estimated population without privately owned vehicles in Auckland. All data sourced from the NZ Census 2018 and presented for each SA2 unit (Statistics New Zealand, 2018).

In the event of future unrest in the AVF, the exact vent location is unlikely to be known prior to an evacuation call (Lindsay et al., 2010; Sandri et al., 2012). As unrest escalates as magma rises, it is thought the vent uncertainty area will reduce (Deligne et al., 2017; Lindsay et al., 2010; Sandri et al., 2012). This will lead to challenges when identifying the population exposure and specific location and size of the required evacuation zones and sequencing of evacuation (e.g. Deligne et al., 2017) and ultimately when an evacuation call should be made. In this paper, a circular buffer from each grid point across the AVF is used to represent the vent uncertainty area. No priori information on the shape of this area is available, hence an unbiased (minimum assumption) circular buffer was chosen. Then, from each vent uncertainty buffer zone, 3 and 5 km are added to model the PEZ and SEZ, with the PEZ incorporating the buffer zone. While we acknowledge the AVF volcanic contingency plan states that the SEZ can be extended to include areas that can become isolated from the eruption (Auckland Council, 2015), these areas have not been included as they are likely small and therefore unlikely to change the results. In this way, changes in

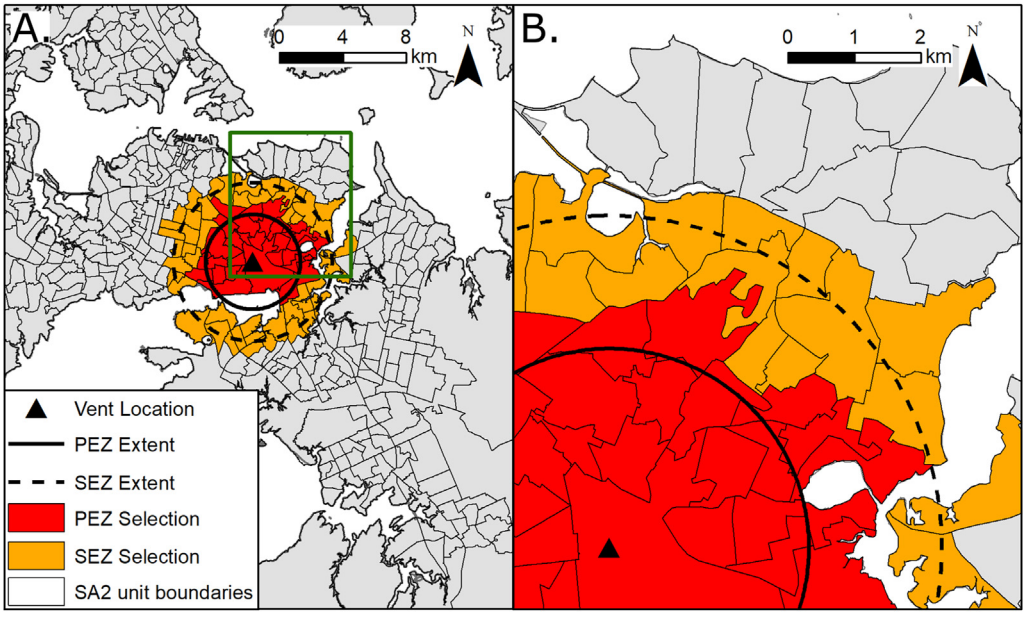

Fig. 4. Example calculation of the process for spatially assessing the SA2 units within each of the primary and secondary evacuation zones. This example shows (A) Wider Central Auckland and (B) PEZ and SEZ boundary conditions for the SA2 units selected to assess the population required to evacuate. The red shaded SA2 units indicate the estimated population required to evacuate from the PEZ. They are those units that are completely within or intersect the boundary of the PEZ from the hypothetical vent. Similarly, the orange zone indicates the SA2 units that are within or intersect the boundary of the SEZ.

population exposure due to vent uncertainty can be better evaluated. To assess the variability in vent uncertainty and the effect on population exposure, we consider vent uncertainty sizes of 0 to 10 km, at 0.5 km increments, for each of the AVF grid points.

3.2. Evacuation phase times

Urbanik et al. (1980), see also Lindell et al., 2020) propose that the time required for an individual resident or transient household to evacuate after incident initiation can be defined as the sum of four time phases (Eq. 2).

$$t_T = t_D + t_N + t_P + t_E \quad (2)$$

Where t_T is an individual or household's total clearance time, t_D is the authorities' decision time, t_N is the evacuation notification receipt time, t_P is the individual or household's evacuation preparation time, and t_E is the individual or household's evacuation travel time.

This study applies the approach presented in Eq. 2 to assess the total evacuation clearance time, and the following subsections outline the approach taken to determine each of the four phases. Ideally, times for each phase could be estimated based on analogue evacuations elsewhere. However, there are no examples of evacuation from volcanic activity in developed countries that could be considered analogous to Auckland in terms of their legislative frameworks and vehicle and public transportation access.

One of the challenges particular to volcanic eruptions is the variable onset time, i.e. the time from initial detection of activity through to eruption. In Auckland, the potential for a stalled eruption and an uncertain vent location add additional complexity (Hopkins et al., 2020; Lindsay et al., 2010; Sherburn et al., 2007). Volcanic eruptions are different to other geological hazards such as tsunami and earthquakes, in that the latter have comparatively short and well understood onset times and modelled extents (e.g. Lindell and Perry, 2012; Sorensen et al., 2020; Wright et al., 2014). However, some characteristics of another natural hazard - hurricane - might lend them to being suitable analogues to volcanic eruptions in the context of evacuations. For example, hurricanes display long and variable onset times compared to tsunamis, and display uncertainty around the event location i.e. where it makes landfall, as well as uncertainty in the area likely to be impacted, and in the eventual magnitude (category) of the event. Hurricane onset time is on a similar timescale of hours-to-days as is expected for the lead-up to an AVF eruption (Blake, 2006; Brenna et al., 2018; Chinander Dye et al., 2014; Kereszturi et al., 2014; Lindell et al., 2007; Sorensen et al., 2020). Finally, similar proportions of the population perceive themselves to be prepared for a future AVF eruption and US hurricane: > 75% of surveyed Auckland residents (Coomer et al., 2015) and between 49% and 76% of households across 5 cities in the US (Blendon et al., 2007; Solutions Pacific, 2018), respectively. On the other hand, there are also obvious differences, such as frequency of occurrence between hurricanes and volcanic eruptions: hurricanes occur annually and their impacts remain in social memory, whereas volcanic eruptions requiring evacuation occur much less frequently and often fall from societal memory, making it difficult to extrapolate hurricane data for evacuations to other hazards such as volcanic eruptions (Marrero et al., 2010).

Due to a lack of data specifically related to volcanic crises in urban environments analogous to Auckland, hurricane data is used here to inform evacuation phase times. Where appropriate, additional data relating to the specific temporal phases of evacuation are also included in the model, for example past experience regarding government issuance of emergency notifications, for example during the COVID-19 pandemic.

3.2.1. Decision time

The decision time is the time elapsed from detection of an incident (t_0), i.e. volcanic unrest in the case of this study, until authorities make the decision to call an evacuation (Urbanik et al., 1980). This is divided into two components: the detection of volcanic unrest from the monitoring team and volcanologists; and the decision to call an evacuation from decision-makers and emergency management.

The detection time is represented using a linear interpolation representing maximum ignorance between 4 and 24 h with 0 and 1 cumulative probabilities of detection respectively. The lower bound of 4 h is based on the 20 min requirement for GeoNet to locate and report earthquakes (MCDEM, 2015), and the time estimate for the monitoring team to convene a meeting to discuss the VAL and publish a volcanic alert bulletin. The upper bound of 24 h is based on the interval between volcanic alert bulletins leading up to the change to VAL 2 during Exercise Rūaumoko (Lindsay et al., 2010).

There is limited published information on the time taken by authorities to make the decision to call an evacuation (Table 1). Estimated quantiles for each of these decisions that are published, and their respective times, were assigned within an exponential distribution (Eq. 3; Bebbington and Zitikis, 2016), by using counterfactual analysis, i.e. could the decision have been much better or worse.

$$P(T \leq t) = 1 - e^{-\lambda t} \quad (3)$$

The value of λ was calculated from the median event resulting in the distribution in Fig. 5. The fitted mean of the exponential is 1/λ. The median time is considered the recent (August 2020) COVID-19 resurgence in New Zealand and subsequent lockdown of Auckland (Trevett, 2020). It is the most recent major event in Auckland to involve crisis decision-making and, as with a future volcanic eruption, the decision making was informed by scientific data and knowledge and required a high level of communication between scientists and local and national officials. The λ values estimated from the 5 cases in Table 1 are remarkably consistent, supporting our contention that the exponential distribution is a

Table 1
Summary of past crisis decision times.

Decision time (hours)	Event, and subsequent action	Source	Cumulative probability of evacuation decision time	λ
2	Hurricane Rita, USA, 2005. Galveston County issued an evacuation notice 2 h after the hurricane warning was issued. (Note that this is likely strongly influenced by social memory and media coverage, given Hurricane Rita occurred just weeks after Hurricane Katrina)	Wu et al., 2012	0.2	0.111
6	COVID 19, Auckland, New Zealand 2020: Time taken to put Auckland back into lockdown following COVID resurgence following positive test of someone in the community.	Trevett, 2020	0.5	0.116
	Indian ocean tsunami, Mauritius, 2004: issuance of evacuation order following the earthquake that – This includes the five hours that elapsed before officials received notice of the event.	Perry, 2007		
24	Exercise Rūaumoko, Auckland Volcanic Field, New Zealand 2008: Participants expressed the view that the call for evacuation was probably a day late; this could have been attributed to a slow passage of information through Auckland Volcanic Science Advisory Group	Cronin, 2008	0.95	0.125
	Hurricane Katrina, New Orleans 2005: Mayor issued evacuation call 24 h after the National Hurricane Center issued the warning.	Lindell, 2008		

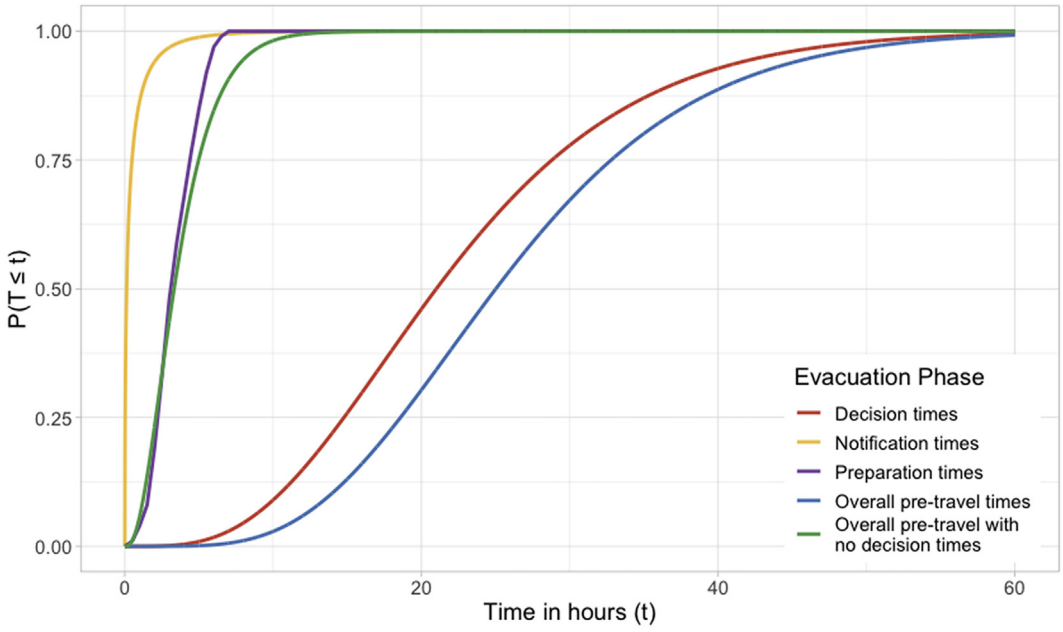

Fig. 5. Evacuation temporal phase curves represented as a function of the proportion of population completed versus time. These are for the decision time (t_D), notification time (t_N) and preparation time (t_P) and the cumulative function for all three stages and the decision and notification times.

good representation of the variability in the decision time, and we will henceforth use $\lambda = 0.116$.

3.2.2. Notification time

The notification time can be characterised as the time taken between the decision being made by authorities and a person receiving the notice to evacuate. When considering a large population, this is typically expressed as a function of time versus the proportion of people needing to be notified. In this study, the function selected to represent notification time was taken from Lindell (2008) (Fig. 5). This function is for a hurricane event with a late change in track, and was informed using evacuation notification time collected for local communities following the 1980 Mt. St. Helens eruption (Lindell and Perry, 2004; Lindell et al., 2007, 2002). This curve represents both broadcast methods (media, authorities etc.) and informal ("contagion") methods (e.g. family, peers) (see also Rogers and Sorensen, 1988). At the time an evacuation decision is issued, notifications are sent via multiple sources, which results in the initial steep rise of the curve.

A New Zealand 2019 emergency management alerts (EMA) survey found that 70% of people surveyed received the mobile phone message alert, which is increased to 77% when including those who were with someone that received the notification (Colmar Brunton, 2020). Of that 70%, 94% received the alert within an hour of the test. This equates to ~72% of people in New Zealand receiving the alert within an hour. This agrees with the notification time curve presented by Lindell (2008) which estimates ~75% of people receive the notification within the first hour from evacuation call issuance, which was hence considered appropriate for this exercise.

3.2.3. Preparation time

Preparation time is the time it takes for individuals or households to prepare to leave their homes after receiving a call to evacuate. This time accounts for pre-evacuation activities such as getting supplies (e.g. food and medication), packing up belongings, shutting down utilities, securing the property and obtaining information from authorities about evacuation centres and routes. The description of preparation activities in the hurricane literature aligns with those expected activities reported for Aucklanders, for example obtaining supplies (Coomer et al., 2015). Given the preference for Aucklanders to evacuate from home, this study therefore assumes all members of a household evacuate at one time. The preparation time is thus considered to include assembly as a family at a given point (home).

Lindell et al. (2020) presents two functions representing the cumulative probability of a household being prepared depending on the location someone received the notification, either "from-home" or "from-work". These was informed by data collected from the six tasks in the 2001 Texas Hurricane Evacuation Expectations Survey (Lindell et al., 2001) to produce the household evacuation preparation time distribution. In any daytime weekday evacuation, most residents would be away from home, many without means of evacuation (car), separated from family and especially children, with whom they would evacuate as a group. Hence the "from-work" function is selected to be conservative as Aucklanders commonly work in areas of the city that are different to where they reside (Fig. 5; Tomsen et al., 2014), and will very probably evacuate as a household (Coomer et al., 2015), which would require them to return home to evacuate for a typical week-day initiated evacuation, which is included in the preparation time.

3.2.4. Travel time

The previous phases can be expressed as functions of the population proportion completing that phase versus time, and as such are assumed to not change based on factors such as the numbers needing to evacuate. In contrast, the evacuation travel time is spatially dependent based on the number of people, their mode of evacuation and the number of available egress routes.

The primary mode of evacuation in Auckland is assumed to be privately-owned vehicles (Auckland Council, 2014; Horrocks, 2008); this aligns with the experience of other developed countries (Cole and Blumenthal, 2004; Lindell and Perry, 1992; Quarantelli, 1980; Tierney et al., 2002). This assumption is based on the high number of vehicles, flexibility in destination choice and ability to take personal belongings given the potential loss (Coomer et al., 2015; Tomsen et al., 2014).

Buses are commonly used for evacuations world-wide (Marrero et al., 2010) and planning for their use has been considered for Auckland during an AVF crisis (Auckland Council, 2014). Tomsen et al. (2014) found that 96% of people in Auckland live within 20 min' walk of

buses making it the most available mode of public transport; particularly given that buses can be redirected during a crisis to otherwise unserviced areas to support evacuations. There are currently 1387 buses in the Auckland Transport network, with a total of 66,554 seats (Auckland Transport, 2020, pers. comm., 20 April 2020). In addition, privately owned coaches can also be used, given the Civil Defence and Emergency Management Group Controller has the authority to seize all required assets if a state of emergency has been declared (CDEM Act, 2002). Of course, this assumes drivers are available and willing to work.

The area with the maximum number people of people without access to vehicles (i.e. the CBD and surrounding suburbs) is close to train stations for routes that extend south or west beyond the AVF. A six-carriage train in Auckland can carry up to 1000 people without luggage, and in theory could allow 10,000–16,000 people per hour to be transported out of the central region of Auckland (Auckland Council, 2014). With the number of available public transport seats, there is likely sufficient capacity to evacuate those without their own vehicles, again assuming sufficient drivers are available and the rail network has not been damaged by unrest phenomena (e.g. ground deformation or earthquakes).

Given the widespread car ownership and preference to evacuate via privately owned vehicles, this study calculates evacuation clearance times using the number of available private vehicles. Coomer et al. (2015) reports 62.7% of Aucklanders surveyed would take one car per household when evacuating and 33.7% would take more than one car. However, this survey does not report on number of vehicles per household. Based on the 2018 census, 30.3% of Auckland household have one vehicle, while 63.1% have two or more (Statistics New Zealand, 2018). Furthermore, additional cars are easily evacuated assets and can be used to transport personal belongings. Hence, to be conservative, it is assumed for our model that all vehicles are used to evacuate. By using the maximum number of vehicles, output analysis will form an upper limit for evacuation travel times. To include the population without personal vehicles in this model, it is assumed they evacuate only via buses. The number of evacuees a bus can transport was estimated as 24, which is derived from the average number of seats across all Auckland buses, assuming an occupancy of 50%. The approximate number of buses required was calculated using the total number of people without vehicles divided by the number of evacuees per bus. The number of buses is added to the number of personal vehicles to subsequently calculate the evacuation travel time. One key limitation is that it relies on bus and driver availability and the re-routing of these within the network.

Usual transport models typically identify the best-route and assume that vehicles drive in a globally optimum way. Sophisticated modelling approaches such as agent-based transportation modelling exist that could be used to model travel times. Agent-based models can be used to modify the behaviour of agents (representing people), allowing them to interact with each other and thus generate congestion in the road network. However, such an approach requires input of substantial human behaviour data for it to reflect realistic conditions, which are not available for our Auckland case study. Nor do validation data exist. In addition, such sophisticated approaches are computationally exhausting and not scalable for the number of scenarios being evaluated as part of this model. Due to these limitations, we instead sought a pragmatic solution for modelling 1000s of people with considerable aggregation at an appropriate level of sophistication for the questions being examined, employing a simplistic geospatial approach.

The applied approach considers the bottlenecks to leaving a region as being the roads that cross the evacuation zone border. This is based on the idea that bottlenecks occur on the major arterial roads as vehicles merge in from surrounding smaller feeder roads. As shown in Fig. 6, the carrying capacity, defined here as the number of vehicles the road can support per hour per lane at free-flow, is less than the collector roads feeding into it, hence we do not need to model the latter as they add no delay. As more roads within the evacuation zone feed into the direct egress routes beyond the evacuation zone border, these are likely the most inundated.

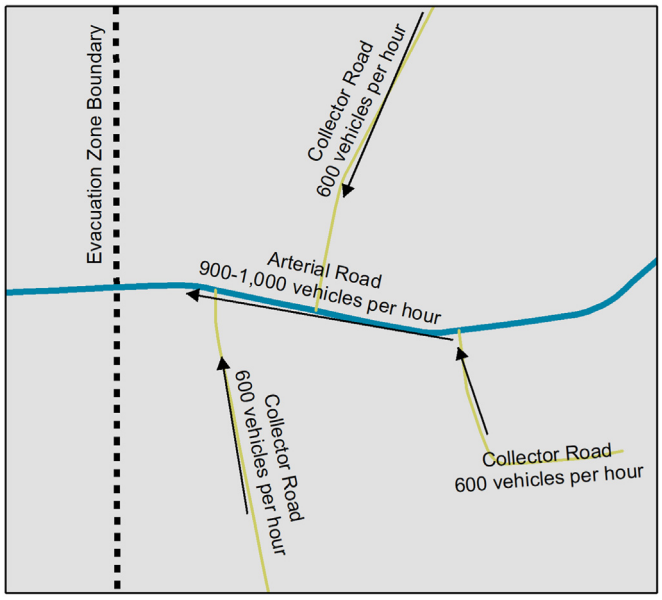

Fig. 6. Schematic illustration of two classes of roads used to evaluate carrying capacity.

The road data used was the New Zealand Transport Agency (NZTA) One Network Road Classification dataset (received on the 18 Oct 2019 from NZTA; refer to New Zealand Transport Agency, 2013). This dataset was filtered based on the NZTA One Network Road Classification to only primary collector, arterial, regional and national routes, thereby removing the smaller access roads (such as residential streets) that feed in and out of the major routes. The number of lanes is also required as vehicle carrying capacity for a road is reported based on the number of vehicles per lane per hour (v/h/ln; Green et al., 2020; Transportation Research Board, 2016). As the NZTA One Network Road classification dataset does not contain the number of lanes, the LINZ 1:50 k centreline dataset, which contains the number of lanes, was spatially joined (downloaded from LINZ 11 Oct 2019). Engineering design standard vehicle carrying capacities for different types of roads considered within this study are presented in Table 2. Under evacuation conditions, the road network is assumed to be operating near-to or at maximum capacity. Based on Transportation Research Board (2016), highways have a free-flow vehicle capacity of 1900–2200 v/h/ln, where there is a vehicle speed variability of 70–100 km/h. The arterial roads have a vehicle capacity of 900–1000 v/h/ln (Green et al., 2020). The range is a result of road structural elements such as presence of central road divides and lane position. No dataset of structural information exists, therefore a range was applied to acknowledge this variability. For residential roads, the vehicle capacity of 600 v/h/ln (Green et al., 2020) was applied as such roads are more consistent with narrower thoroughfares, obstructed paths and reduced vehicle speeds. While we acknowledge this approach relies on many assumptions, if a road dataset containing each individual road's vehicle capacity becomes available, this analysis can be updated.

For each point across the AVF Grid, the capacity was summed for those roads that intersected the SEZ boundary (see. Fig. 4). This builds on the Tomsen et al. (2014) methodology for assessing the ease of evacuation for population based on vehicles and egress routes, and translating the ease of evacuation into a time for the evacuation to complete. The travel time is subsequently calculated using (Eq. 4).

$$t_T = \frac{\sum vehicles\ in\ evac\ zone}{\sum vehicle\ capacity\ of\ egress\ routes} \quad (4)$$

Table 2
Road types with vehicle carrying capacity applied in this study.

Road type	Vehicle capacity (v/h/ln)	Reference	NZTA one network road classification[a]
Highways	1900–2200	Transportation Research Board, 2016	National
Arterial routes	900–1000	Table 6.1 in Green et al., 2020	Arterial, regional and primary collector
Residential access and collector roads[b]	600	Table 6.1 in Green et al., 2020	Local and secondary collector roads

[a] New Zealand Transport Agency (2013).
[b] Default value when no highways or arterial roads are identified as egress routes.

To account for the variability in the vehicle capacity of the roads summarized in the ranges in Table 2, the capacity is simulated from a uniform distribution, within the range limits provided by the road class. If there is no egress route identified, the capacity is set to 600 as it is assumed the evacuating population would need to evacuate via the smaller residential and collector roads. In addition, an evacuation can cause a decrease in road capacity of 10–20%, primarily as a result of downstream congestion (Yin et al., 2020). This range is also simulated as a uniform distribution. Each of these distributions are stochastically sampled ($n = 1000$) for each vent location and evacuation zone size. This allows a distribution of evacuation travel time to be calculated across all vent locations and ranges in road carrying capacities, in order to quantify the uncertainty involved. Table 3 contains a summary of the output travel times for all AVF grid locations and accounting for variability vent uncertainty size.

One limitation with this approach is that it assumes the roads are at free-flow (q_{max} in Fig. 7), yet actual flow will vary throughout the evacuation. It is unknown what the effects of congestion will be during a future crisis. However, to assess the potential changes in evacuation travel time due to road network congestion, we consider evacuation capacities reduced to 2/3 and to 1/3 of the free-flow capacity. This results in the median travel time for a 5 km radius evacuation zone to increasing from 0.8 to 1.2 and 2.5 h, for the 2/3 and a 1/3 free-flow capacity respectively.

3.2.5. Evacuation clearance time analysis

Following the approach presented in Eq. 2, stochastic sampling (n = 1000,000) from each of the first three phase functions are summed to form a pre-travel time distribution, which is the blue curve in Fig. 5. This is summed with the spatial variable travel evacuation time to produce a spatial model for Auckland for a total evacuation clearance time for any given vent location and evacuation zone radius.

The decision time (t_D) is a single value for all of the evacuation zones, determined by the time taken to call the evacuation from incident detection (t_0). In contrast, the three other phases are represented as probability distributions for the time taken for the at-risk population to have completed that phase. Reducing the average decision time will reduce the variability in the overall evacuation time, which would therefore change the shape of the total pre-travel time function, where t_D would be a constant which is added to the household individual pre-travel time (Fig. 8). Given the cumulative pre-travel distribution, and noting the strong influence on this of the decision time, the percentiles completing the pre-travel phase in 24, 36 and 48 h are 46%, 82% and 96% respectively. These commonly used time intervals are selected here only to illustrate the pre-travel distribution. For pre-operational scoping of such an approach, the desired percentile would be selected by decision-makers to reflect their desired risk tolerance, and the time required calculated from it. When presenting the evacuation clearance times below, we apply a pre-travel time of 36 h, the 82nd percentile value, to demonstrate the approach.

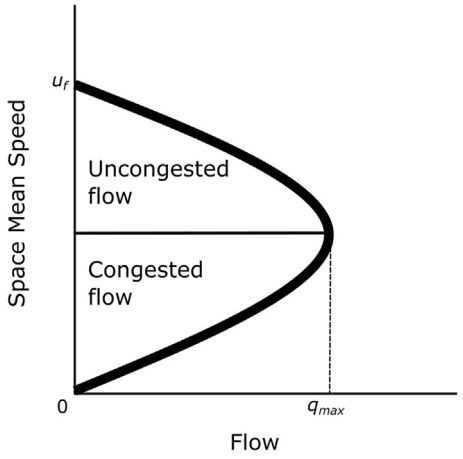

Fig. 7. Space mean speed versus volume (from Garber and Hoel, 2010).

Up to this point, the presented methodology has considered the clearance time as independent from the probability of the next AVF vent location, thereby assuming a uniform distribution of vent occurrence within the AVF. In the supplementary materials we present the method and results for weighting published models of AVF spatial intensity for future vent location (Bebbington, 2015, 2013; Bebbington and Cronin, 2011) with respect to the evacuation travel time (t_E) to assess how the vent likelihood changes the travel time distributions across the AVF.

Table 3
Evacuation travel times for a range of radial distances across all AVF grid locations. Note: 5 km is added to the vent uncertainty buffer distance to form a series of combined evacuation zones (PEZ + SEZ) with increasing vent uncertainty.

Vent uncertainty buffer distance	Evacuation travel times (hours – 1 dp)		
	10th percentile	50th percentile	90th percentile
0 km	0.1	0.8	1.4
1 km	0.2	1	1.7
3 km	0.5	1.3	2
5 km	0.8	1.6	2.3
7 km	1.1	1.9	2.8
10 km	1.4	2.4	3.5

4. Results

4.1. Population exposure

The results for population within the PEZ (which includes the vent buffer zone), SEZ and the combined evacuation zone (sum of PEZ and SEZ) for a given vent location are presented graphically and spatially for Auckland Fig. 9. Note that for this initial analysis the vent buffer zone is set to 0 km, i.e. uncertainty in vent location is not included. Some overarching trends are immediately visible. The median (assuming all vent locations are equally likely) population count within the PEZ is approximately 53,000 people, with the maximum population at approximately 168,000 (Fig. 9a). The areas where the PEZ covers the largest population are around the densely populated residential suburbs in central Auckland (see the map in Fig. 9a). The SEZ covers a wider area,

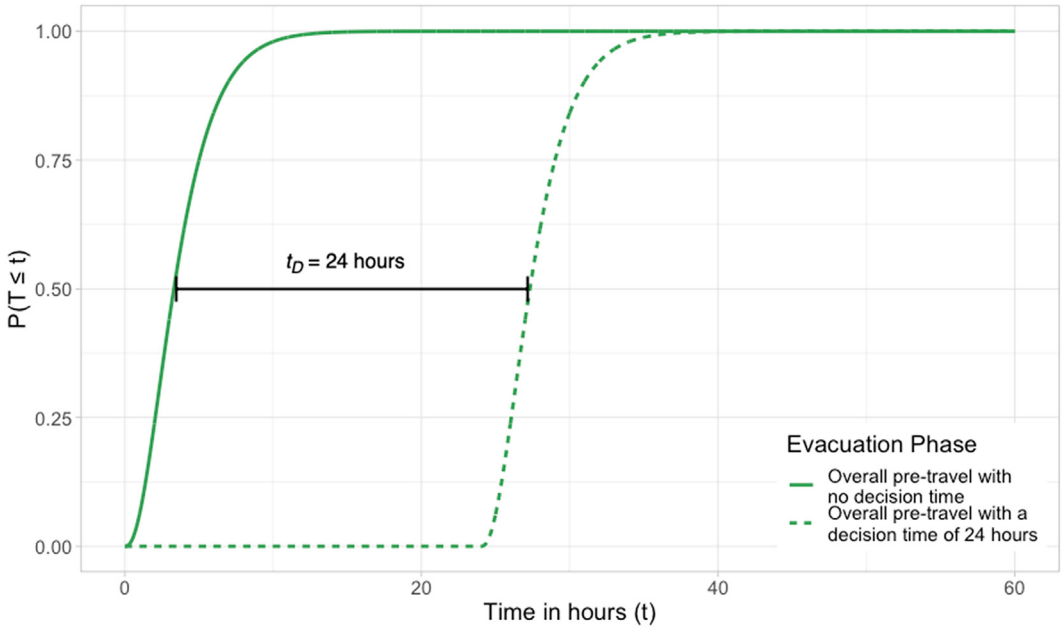

Fig. 8. Demonstrating how a fixed decision time (t_D) of 24 h is added to the household level pre-travel time distribution (green line in Fig. 5) to reflect population completion of the pre-travel phase for an event.

and as such captures a greater population: the median population in the SEZ is approximately 69,000, and the maximum population approximately 176,000 (Fig. 9b). This wider coverage means that, in comparison to the PEZ, there are also fewer vent locations that result in no people in the SEZ (~525 compared to ~825 for the PEZ; Fig. 9b and a, respectively). Fig. 9c presents the results for population exposure in both evacuation zones (i.e. PEZ + SEZ), henceforth referred to as the combined evacuation zone. The median total population identified as being within the combined evacuation zone is 131,000, with 320,000 identified as the maximum. The vent locations that yield the greatest populations within the combined evacuation zone are located in the densely populated residential suburbs in central Auckland (see map in Fig. 9c). There are 22 vent locations, which is <1% of the overall AVF size, that result in more than 300,000 people in the combined evacuation zone. 515 (all offshore) of the 3312 vent locations (~16%) within the AVF have a minimal population (⟨10,000) within their total evacuation zone. The values presented in Fig. 9 do not account for vent uncertainty. In order to evaluate how vent uncertainty affects the population exposure, we added vent uncertainty buffers of 0 to 10 km to the PEZ. This reflects a more realistic possible future crisis management scenario in which an evacuation may have to be called before an exact vent location is known. The population exposure within the combined evacuation zone (PEZ plus SEZ) for four different vent uncertainty buffer sizes (1, 4, 7 and 10 km) are presented graphically in Fig. 10 and spatially for Auckland in Fig. 11.

As shown in Fig. 10, the population exposure increases when the buffer zone representing vent uncertainty increases; this is not unexpected, given that the required evacuation zone covers a wider area of the city. The maximum exposed population considering 1 km vent uncertainty is ~375,000, whereas with a vent uncertainty area of 10 km the maximum is ~1.1 million. For all uncertainty buffer radii, the vent locations that produce the maximum values are in and around the CBD. Of course, the minimum population exposed also increases with vent uncertainty. This is evidenced by the minimum population exposed for the 7 and 10 km vent uncertainty buffers being identified as ~60,000 people and ~ 225,000 people respectively, compared with <200 people for both the 1 and 4 km vent uncertainty buffers. The vent locations for each vent uncertainty buffer size that produce the minimum population exposed are offshore in the north-eastern extent of the AVF. Here, increasing the vent uncertainty buffer from 4 to 7 km creates a significant increase to the evacuation zone, which extends it into onshore areas, thus encompassing a greater proportion of the population. The vent locations producing these minimum population exposures are all located within the +5 km AVF buffer extent used to constrain the study area. A key observation is that the increasing vent uncertainty smooths the spatial variability in population exposure (Fig. 11).

In addition to understanding the overall spatial variability in population exposure, it is important to consider the population that does not own a vehicle to self-evacuate, as it is assumed these people will require support via public transport. Our analysis show that vents that result in a combined evacuation zone that intersects the CBD will result in the greatest exposure of people without vehicles, due to the high population density and lower vehicle ownership in the CBD (Fig. 12). The distribution of people without a vehicle vs. overall population within the combined evacuation zone considering a range of vent uncertainty buffers can also be calculated (Table 4). This shows the maximum proportion of the population that do not own a vehicle is 19%, when the vent uncertainty is less than or equal to 5 km, however the 50th percentile is 6–8% depending on the vent uncertainty buffer size, for a uniform vent distribution across the AVF.

By visualising the relationship of total population vs. population without vehicles based on the region in Auckland (Fig. 1) in which the vent is located, clear trends can be observed (Fig. 13). There is a monotonic relationship between total population and population without vehicles, i.e. less total people equates to less population without vehicles. However, there is a bi-level division in the relationship for vents located in the CBD and inner central suburbs and some of the North Shore. This division is due to the possible vents located in these two regions resulting in a combined evacuation zone that would encompass the CBD, where there is the greatest ratio of population without vehicles, but which also includes the highest overall population density.

4.2. Evacuation clearance time

The median evacuation clearance time (ECT) for a 5 km radial evacuation zone considering free-flow vehicle capacity is presented spatially for Auckland in Fig. 14. The longest evacuation clearance times occur when the vent location lies within predominantly residential areas

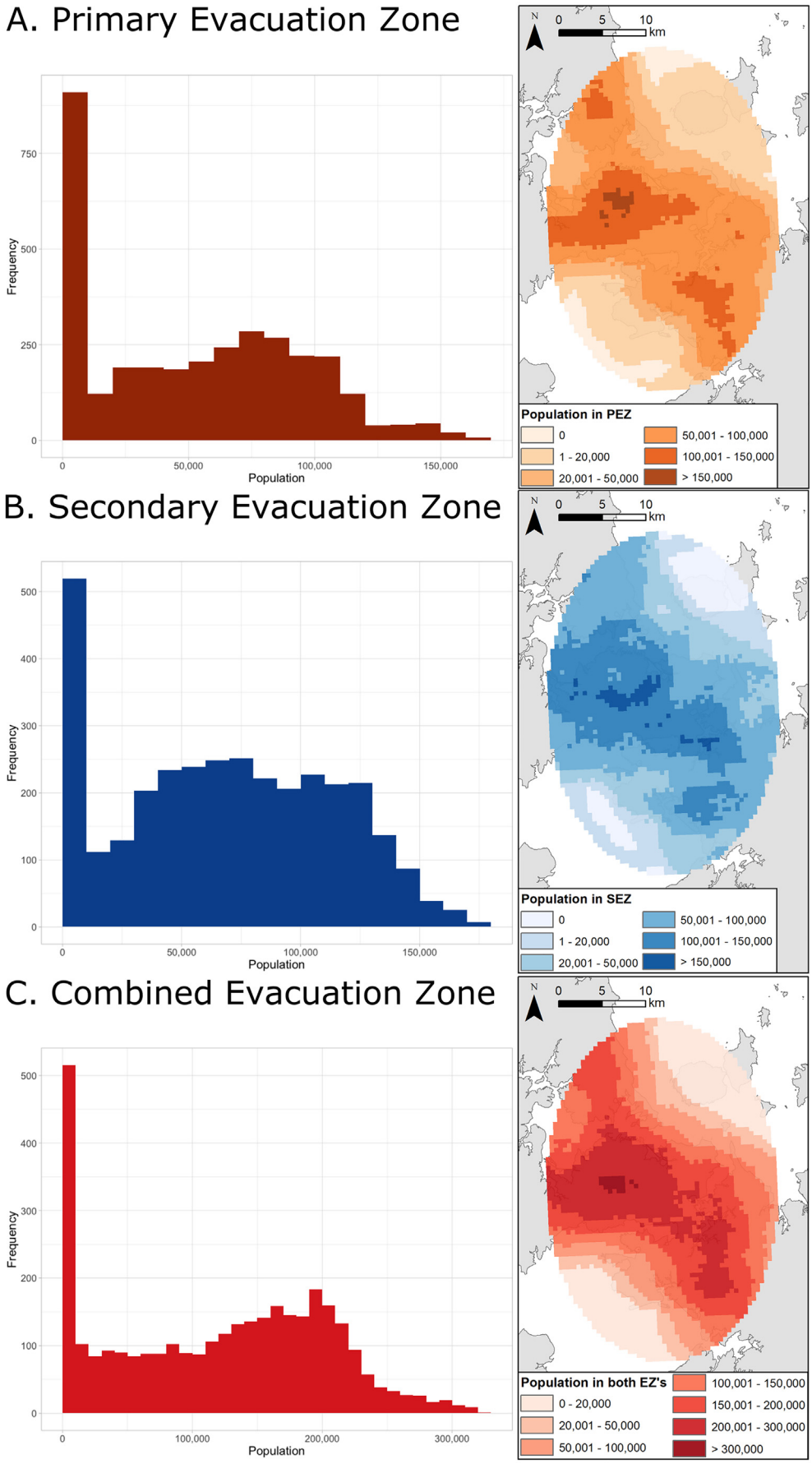

Fig. 9. Population exposure from an eruption in the Auckland Volcanic Field from any given vent within the AVF for (A) PEZ, (B) SEZ and (C) Combined evacuation zones (PEZ + SEZ). Note: for the maps, the cell value is the population within the evacuation zone for a vent location within that cell. For these initial analyses the vent buffer zone is set to 0 km.

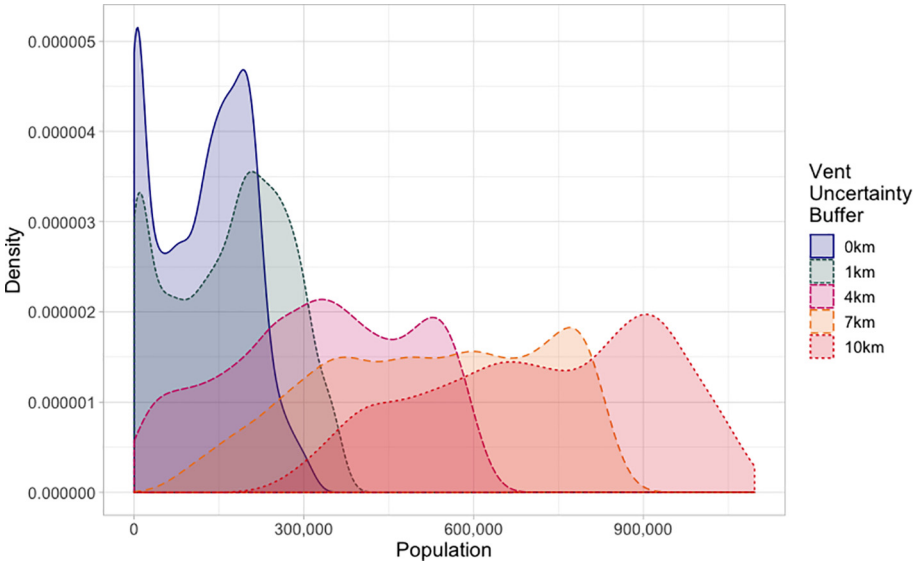

Fig. 10. Density plot of population within the combined evacuation zone (PEZ + SEZ) for vent uncertainty buffers of 0, 1, 4, 7 and 10 km from all AVF grid locations.

with the highest population density. However, at the free-flow vehicle capacity, there is very little spatial variability across Auckland, with a median clearance time of 36.8 h and a maximum of 40.3 h (Fig. 14; Table 5). This is because when considering free-flow traffic conditions the overall evacuation clearance time is predominantly influenced by the pre-travel phase, primarily the decision time, which will be a single value across the entire evacuation zone.

When there is a change to the vehicle flow capacity due to potential congestion, there is a noticeable increase in clearance times. However, clearance times are still dominated by the pre-travel time. The 2/3 free-flow capacity increases the median and maximum clearance times to 37.2 and 42.5 h, respectively (Table 5). The median and maximum clearance times for the 1/3 free-flow capacity are 38.5 and 49 h respectively. The clearance time is largest if an evacuation occurs from the densely populated areas of the city, especially where there is limited access to high vehicle carrying capacity egress routes such as highways. This is especially clear in the eastern part of the city, where there are no highways defined as egress routes out of the evacuation zone. Here, the geography of east Auckland would require people to evacuate to the south-west to reach the highways, as the area is bound by the coastline on the other sides. This is a common dilemma for urban environments built along the coast that are faced with the need to evacuate, e.g. Naples, Italy (Charlton et al., 2020).

We examined how vent uncertainty affects the evacuation clearance times. Table 5 contains a summary of the evacuation clearance times for all AVF grid locations and accounting for variability in road carrying capacities. This shows there is a marginal decrease in clearance time (< 6 h) as vent uncertainty decreases from 10 to 0 km, beacuse that while the population needing to evacuate decreases, so does the egress capacity to support those evacuating from the smaller evacuation zone.

Examining the difference between the evacuation clearance times for different vent uncertainty sizes highlight where across the AVF the largest changes in clearance times are. The difference in clearance time also shows potentially where, during a crisis, officials may choose to wait longer for increased certainty around vent location, thus reducing the number of people needing to evacuate. However, while waiting does have its benefit in reducing evacuation times, the eruption likelihood may simultaneously be increasing (Bebbington and Zitikis, 2016), reducing the time available. Fig. 15 presents the difference in clearance times between the 0 and 10 km vent uncertainty buffer distances with consideration of different vehicle flow capacities.

Due to Auckland's geography, the difference in the clearance times is primarily due to the provision of egress routes. With a larger evacuation zone, there are a significant number of possible vent locations in the field along the central corridor of the city whose evacuation zones have the potential to intersect both the eastern and western coastlines, resulting in identified evacuation routes that can only go north or south (Fig. 16).

5. Discussion

5.1. Potential application of the model

We have developed a volcanic crisis evacuation-support model that yields the following key outputs: number and spatial distribution of people that would need to be evacuated, number and spatial distribution of people who would likely need public transport support to evacuate, and evacuation clearance times and their spatial distribution. Such outputs can support emergency managers with risk management decisions before and during a volcanic crisis, particularly in contexts where the exact future vent is unknown. Understanding the number and spatial distribution of people exposed can support response and welfare logistics such as preparing evacuation shelters and emergency supplies. Understanding the number and spatial distribution of people without a personal vehicle can support the planning for use of public transport for evacuation. Before a crisis, an understanding of evacuation clearance times can be used to support pre-event planning. For example, the regions that are estimated to require more time to clear could be identified and considered for measures such as contra-flow, a practise commonly carried out in the US during hurricane evacuations that allows greater capacity to evacuate in a specific direction (Clark et al., 2020). This would likely require considerable pre-event response planning and preparation by emergency management, police, traffic management and other organisations.

During a crisis, model outputs could inform the decision of when to evacuate, for example by combining model outputs with quantitative volcanic hazard models and cost-benefit analysis to identify the optimum time to call an evacuation (Bebbington and Zitikis, 2016; Marzocchi and Woo, 2009, 2007; Sandri et al., 2012; Wild et al., 2019b). As vent uncertainty changes, and as the crisis develops, the model could be run in real time to assess population exposure and clearance times to support decision-makers.

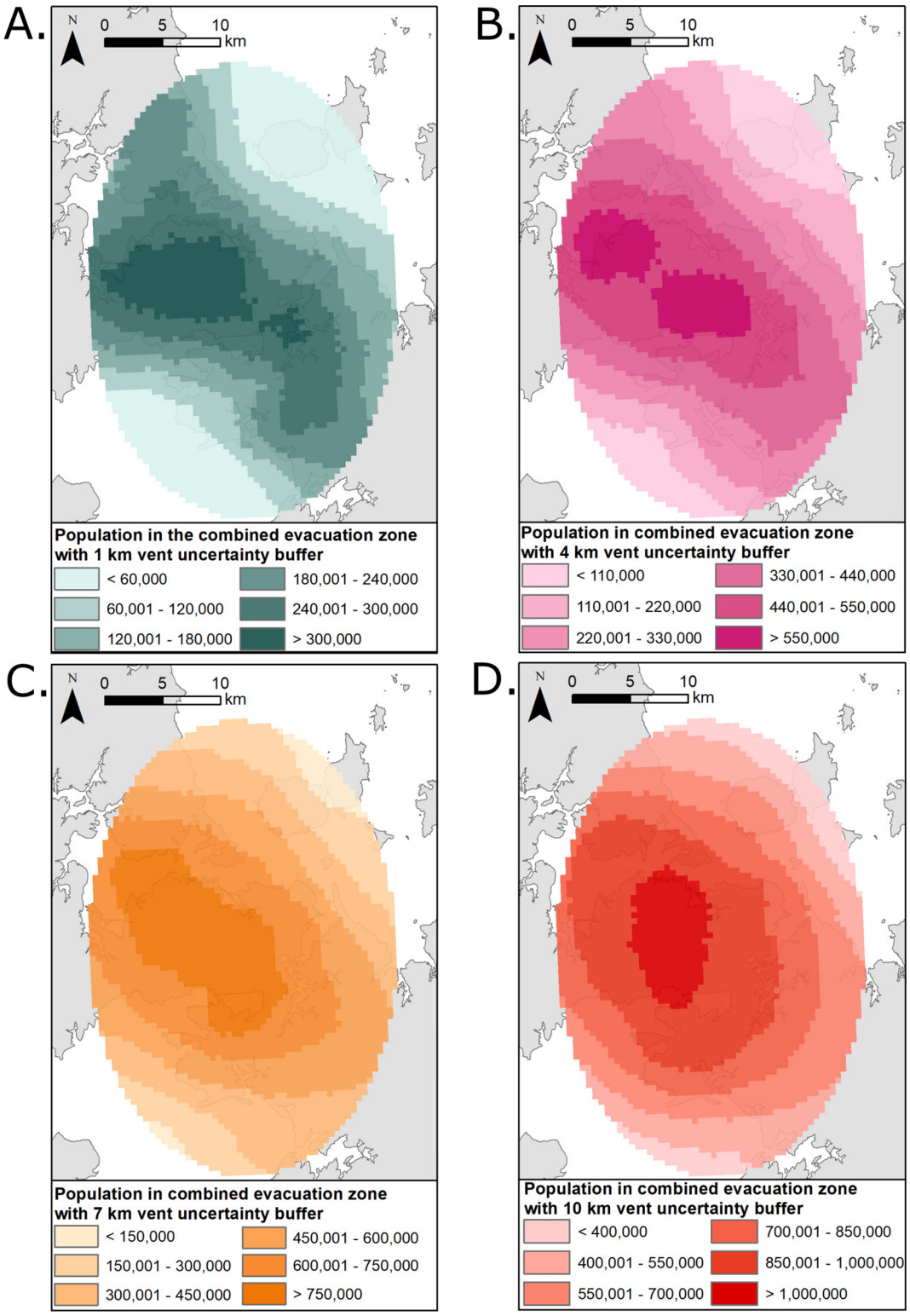

Fig. 11. Population exposure within the combined evacuation zone (PEZ + SEZ) from an eruption in the Auckland Volcanic Field from any given vent within the AVF with vent uncertainty buffers of (A) 1 km, (B) 4 km, (C) 7 km and (D) 10 km. Note: the cell value is the population within the combined evacuation zone for a vent location within the cell.

Future development could consider applying a factor-of-safety value to the outputs of the model to inflate the clearance times if there is a desire to apply a level of conservatism dependent on emergency management and political risk tolerance. Any suitable factor is likely an increasing function of the density of vehicles on each evacuation route.

The conceptual framework presented here could be modified to work for other hazards, such as tsunami and flood. The inputs can be modified by changing the spatial resolution of population data, adapting the approach to consider different policies and using alternate hazard extents. Alternative clearance time model approaches could also be

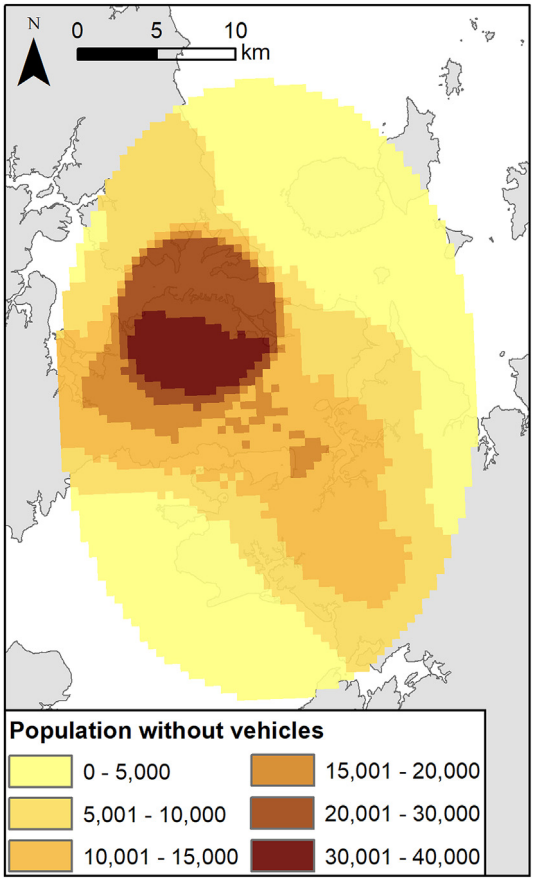

Fig. 12. The number of exposed people in the combined evacuation zone (PEZ + SEZ) without access to a private motor vehicle, for all vents within the AVF. Note: the cell value is the population within the evacuation zone for a vent location within that cell.

employed, including agent-based models, when/if appropriate data is available.

5.2. Application of the model to support evacuation in a future AVF eruption

Our application of the model to a future AVF event sheds some light on considerations for an evacuation in Auckland. Results from our study indicate that, regardless of the future vent area, it would take between 37 and 40 h to clear a 5 km evacuation zone (PEZ + SEZ with no vent uncertainty). Those times are based on the model assumption of free-flowing road carrying capacity; clearance times increase to a maximum of 49 h when egress road carrying capacity is reduced to a third to represent congestion. As part of Exercise Rūaumoko, it was reported officials estimated that they required 48 h forewarning to plan for and then carry out an evacuation (Lindsay et al., 2010). Our study suggests that less time might be sufficient for an evacuation of some areas in Auckland, for example in the south.

While a future vent in the central densely populated CBD and inner central suburbs results in the largest population exposure, limited egress routes and the geography of Auckland also play a role in clearance times. However, a vent located in or around the CBD would result in the largest requirement for public transport, given the comparatively low private vehicle ownership by household in those areas. Indeed, a possible vent in the centre of the city could require more bus trips than there are buses in Auckland; careful planning by emergency management and transport authorities would be required to manage the public transport trip requirements. An example strategy could be employed using buses to shuttle evacuees to train stations beyond evacuation zones, and then using trains to subsequently take people to evacuation shelters. However, this could restrict the use of other evacuation management strategies such as contra-flow.

The two main contributing factors to the overall clearance time were revealed to be 1) the decision time (t_D), namely the time officials take between detectable volcanic unrest that may require an evacuation and calling an evacuation, and 2) the level of congestion of the road network during an evacuation. The decision time is added to the other pre-travel time distributions for notification (t_N) and preparation (t_P) phases (Fig. 8). Reducing the decision time would of course reduce the overall time to complete the pre-travel phases. In our study a ratio of free-flow carrying capacity was used as a proxy for congestion, with the worse-case congestion ratio used being 1/3 free-flow carrying capacity. While many studies have noted the impact congestion can have on evacuation travel times (e.g. Lindell and Prater, 2007; Moriarty et al., 2007; Na and Banerjee, 2019; Tomsen et al., 2014; Yin et al., 2020), in the absence of data to determine a suitable 'congestion' ratio 1, 2/3 and 1/3 were applied in this study to assess the potential changes in evacuation travel time. An informed rationale for selecting a congestion ratio to enable more accurate estimation of travel times would require driver behaviour factors to be incorporated in-depth traffic modelling for Auckland from an AVF eruption scenario (e.g. Afzal et al., 2019), to reflect the less than ideal conditions under which the traffic will be moving. Although we applied a high-level geospatial approach to modelling, our travel time (t_T) results of <1 to 10 h (depending on free-flow capacity reductions) are consistent, despite the differences in methodology, with the 1 to 9 h for intra-regional evacuation obtained by Tomsen et al. (2014). Additionally, weighting travel times by the spatial vent likelihoods presented in various past models revealed that the median travel times change by less than 0.5 h, which has negligible impact on the overall evacuation clearance time distribution (Supplementary material).

An interesting comparison can be made with hurricane evacuation clearance times in the US. These have been reported as 2 to 29 h in Texas and 9 to 24 h in North Carolina, where the ranges of both are largely due to the number of people evacuating (Wolshon et al., 2005). Evacuation clearances times for some large populated centres with potentially challenging routes can be significantly greater. For example, it is thought that New Orleans (with a population of 1.3 million and limited evacuation routes) requires 72 h, and Miami 84 h to evacuate (Chinander Dye et al., 2014). In the analysis for the AVF, the longest maximum clearance time we calculated was ~55 h, for an evacuation of 1.1 million people from an evacuation zone with a 15 km radius (PEZ + SEZ plus 10 km vent uncertainty buffer), using a 1/3 free-flow capacity for the travel time. Overall, our model predicts that although evacuation times are comparable for situations with large number of people evacuating (> 1 million), for smaller numbers of evacuees it may take longer to evacuate in Auckland than in the US in response to hurricanes. These differences likely to reflect differences in decision time, access to transport, and possibly compliance, due to hurricanes in the US being more tangible and visible than volcanic eruptions in Auckland.

Table 4
Ratio of population with no vehicle vs total population exposure for increasing radial distances across all AVF grid locations.

Vent uncertainty buffer distance	Population with no vehicle vs total population exposed			
	10th percentile	50th percentile	90th percentile	Maximum
0 km	0.027	0.057	0.140	0.190
1 km	0.033	0.057	0.121	0.190
3 km	0.039	0.059	0.104	0.190
5 km	0.043	0.063	0.095	0.190
7 km	0.050	0.073	0.090	0.109
10 km	0.054	0.076	0.084	0.097

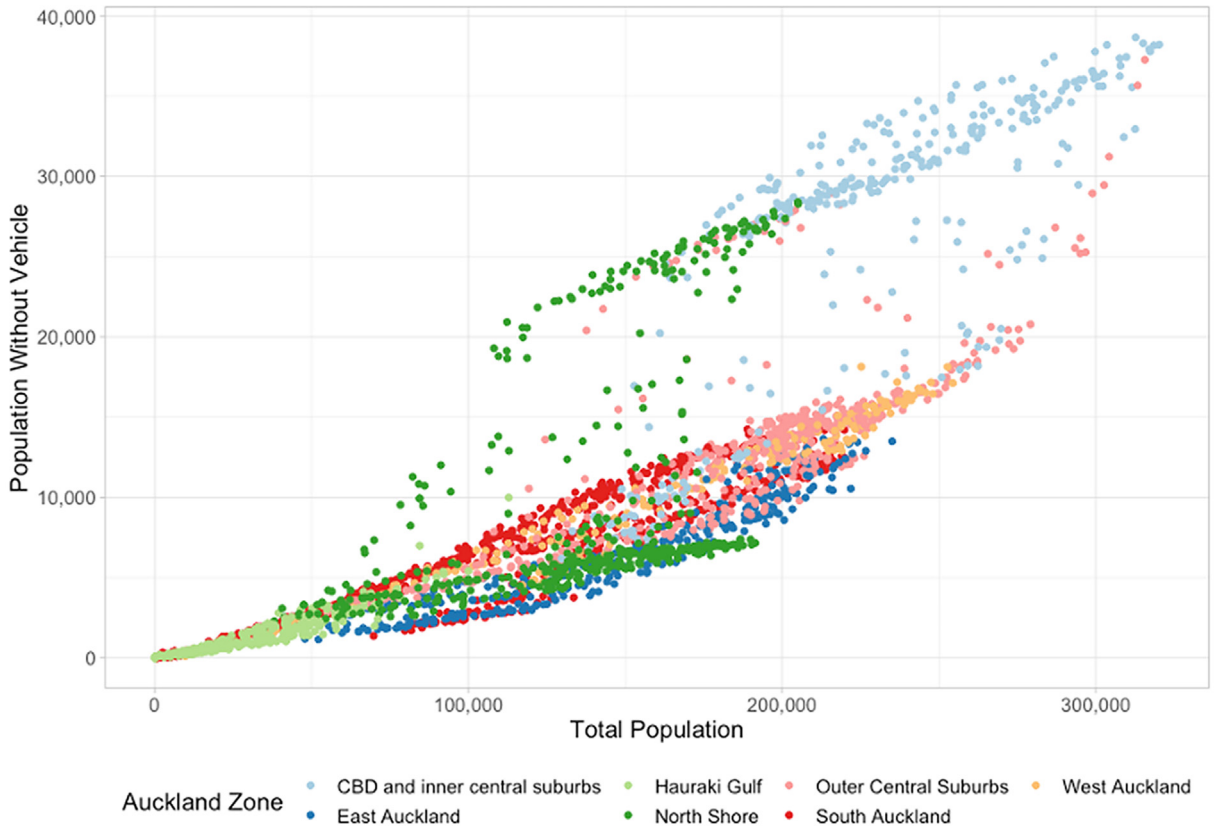

Fig. 13. Total population vs population without access to private motor vehicles within the combined evacuation zone (PEZ + SEZ), with no vent uncertainty, for all AVF grid vent locations.

Ideally, to allow sufficient time for the affected population to get to safety, an evacuation call is required when the impact from the hazard, whether it be volcanic eruption, hurricane landfall, or another, still remains uncertain (Lindell et al., 2007; Lindsay et al., 2010; Marzocchi and Woo, 2007). Hurricane evacuations in the US have been called prior to the National Hurricane Center issuing a warning (Sorensen et al., 2020), which are typically issued 36–48 h prior to landfall (Chinander Dye et al., 2014; Lindell et al., 2007; Sorensen et al., 2020). A similar scenario could potentially occur in Auckland, with non-hazard-related pressures (such as political, media and economic factors) contributing to the decision-making (Wild et al., 2019a). This highlights an additional complexity involved in making the decision to call an evacuation. Given the strong influence of the decision time on the overall clearance time, the ability to make decisions promptly on receipt of scientific evidence of volcanic unrest and a potential eruption could significantly lower the overall evacuation clearance time required.

Based on the evacuation clearance times in this study (Table 5), the difference in clearance time between the 10 and 0 km vent uncertainty sizes is less than the fastest magma ascent times from detection to eruption for the AVF of <2 h based on worst-case magma ascent rates presented in Blake (2006). Hence, even in the worst case, the larger (more uncertain) zone can likely be evacuated in less time than would be taken waiting for additional information to reduce the size of the zone. This indicates it could be beneficial to commence an evacuation as soon as the risk tolerance threshold is met, potentially evacuating far greater numbers than required, rather than wait to localise the vent location. However, this is likely a politically unfavourable option as it would require many more evacuees than would result from waiting for the vent uncertainty to reduce (Bebbington and Zitikis, 2016; Chinander Dye et al., 2014). There could also be welfare and logistical issues with sheltering and supporting such a large number of people.

The evacuation phase time curves applied in this model assume total compliance by evacuees. Our application for the AVF does not consider reluctance by individuals to evacuate, an issue observed globally in past events including the 1996, 2004 and 2010 eruptions of Merapi (Jumadi Heppenstall et al., 2018; Lavigne et al., 2018; Mei and Lavigne, 2012), 2010 Eyjafjallajökull eruption (Bird and Gísladóttir, 2018), 2005 Cordón Caulle eruption (Elissondo et al., 2016) and 1991 eruption of Mt. Pinatubo (Tayag et al., 1996), as well as in the US from hurricanes (Kang et al., 2007; Lindell and Prater, 2007). There are many reasons individuals do not evacuate including: reluctance to leave house, property and animals; limited experience of the hazard and impact leading to poor risk perception; and religious grounds (Blong, 1984; Cola, 1996; Lindell and Perry, 1992; Tobin and Whiteford, 2002). In the event of a significant non-compliant population during the next AVF event, the evacuation clearance times presented here may be a severe underestimate, especially if additional actions such as police door-knocking are required. A survey conducted in Auckland during Exercise Rūaumoko reported 93.6% of participants said they would leave on receiving the evacuation call if they were located within the evacuation zone (Horrocks, 2008), which would be a larger percentage than observed elsewhere (e.g. Baker, 1991; Dow and Cutter, 2002; Lindell et al., 2005).

An interesting consideration that has arisen during our study is how to model the possibility of concurrent hazards - for example evacuation in an AVF crisis during a severe weather event or indeed during a pandemic, which can limit transportation options and/or restrict egress routes. A mass evacuation during a community outbreak of the COVID-19 pandemic for example has the potential to be logistically challenging, especially with regards to social distancing on transportation and in welfare centres to contain the spread of any illness. This challenge is highlighted by the measles outbreak in one of the evacuation

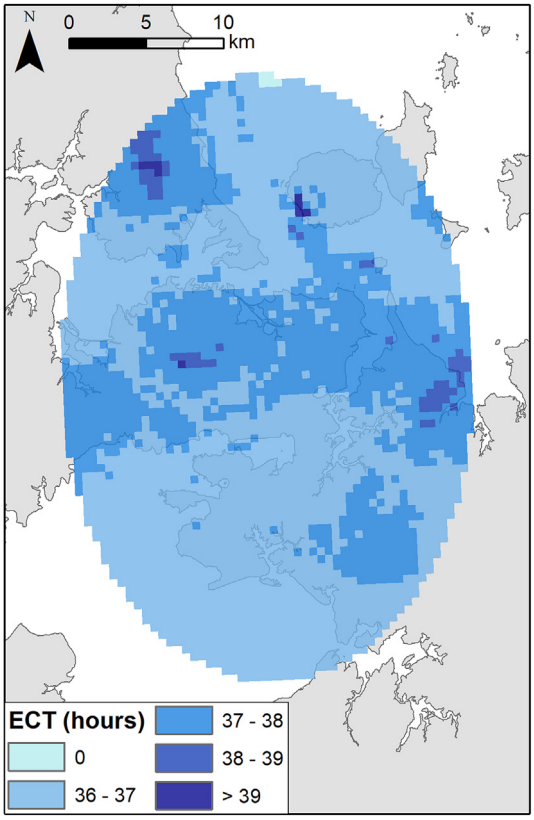

Fig. 14. Evacuation clearance time in hours for private owned vehicles for an eruption from any given vent within the AVF evacuating a 5 km radius with free-flow vehicle capacity. The clearance times use a pre-determined pre-travel time of 36 h. Note: the cell value is the evacuation clearance time for the population within the evacuation zone for a vent location within that cell.

centres following the 1991 Mt. Pinatubo eruption (Bautista, 1996; Floret et al., 2006). A range of measures would need to be considered and put in place to support mass evacuation during a pandemic (Sakamoto et al., 2020). Recently a tsunami evacuation was undertaken in New Zealand whilst under COVID-19 restrictions, in response to a large earthquake centred ~1000 km northeast of the North Island. In that case, officials stated that the civil defence evacuation order overrode the COVID-19 restrictions (Bay of Plenty Emergency Management Group, 2021; NEMA, 2021). It should be noted that the areas notified to evacuate were only under level 2 of New Zealand's 4 tier COVID-19 alert system, which recommends increased vigilance and social distancing but no stay at home measures (COVID-19 Group, 2021). In terms of our application to the AVF, it should be possible to model an evacuation during a concurrent hazardous event such as a pandemic. For example, public transport capacity could be reduced to allow for social distancing on buses and trains, and possible reticence of the population to travel on public transport. Decision time could also be extended to allow for the additional considerations that would be likely required.

The model could also be modified to accommodate specific limiting factors that could affect an evacuation. For example, precursory activity may damage roads, there may be limited emergency shelters, or prioritisation of an evacuation destination may be desirable. In the event of a future AVF event for example, it may be preferable to direct evacuations only to the south, as an eruption may lead to impairment of critical infrastructure, such as transmission lines, resulting in power supply and other utilities being cut off to the north of Auckland (Deligne et al., 2017). This risk might make an evacuation north impractical, as the region would have reduced infrastructure support for power and other dependent services including telecommunications, water-supply and sewage. Identification of these potential issues allows for their consideration in developing pre-determined plans that can be used during an evacuation. Such limiting factors can be included in a future application of our model by only allowing, or by prioritising egress routes in a southward direction.

Further consideration could be given to the size of the evacuation zone in a future AVF eruption crisis. At present the PEZ and SEZ evacuation zones as defined in the Volcano Contingency Plan (Auckland Council, 2015) are informed by the likely and possible base-surge extent, which are thought to be 3 and 5 km from the vent, respectively. However, Brand et al. (2014) found that base-surges could extend as far as 4–6 km from the vent in the AVF. These larger extents could easily be modelled to assess population exposure, by reading off the data and figures presented here. For example, if the SEZ was extended from 5 to 6 km radius around the vent, then looking at the 1 km uncertainty buffer (now the zero uncertainty case), this study finds that while the increase would result in a greater number of people needing to evacuate, especially for vents in and around the CBD and inner suburbs, there would be minimal effect on the total evacuation clearance time.

In a future AVF crisis, vent location likelihood should be considered when assessing the Auckland population exposure and evacuation clearance times. However, as noted above, currently available spatial vent models do not have a significant effect on the outputs of our model. However, once unrest data become available from the monitoring network the vent spatial probability will no longer be uniform (Marzocchi et al., 2008; Selva et al., 2012). The Lindsay et al. (2010) AVF Bayesian Event Tree for Eruption Forecasting application illustrated how this principle of combining prior spatial data with monitoring data can be applied, although the prior distribution used there was spatially uniform.

The approach presented in this study made use of circular buffers to assess changes in evacuation clearance time due to vent uncertainty. This is the only possible approach in applications such as this carried out during periods of quiescence, due to the absence of monitoring data to suggest spatial bias in vent location. Our model could be adapted as needed for use during crisis response, for example by assessing population exposure and travel times based on differently shaped regions representing the vent uncertainty area, similar to those presented in other studies for Auckland (e.g. Deligne et al., 2017). Ideally, near-real time calculation of population exposure, access to vehicles and evacuation clearance times would be carried out to support decision-makers.

Table 5
Evacuation clearance times for a range of radial vent uncertainty buffer distances across all AVF grid locations. Note: 5 km is added to the vent uncertainty buffer distance to form a series of combined evacuation zones (PEZ + SEZ) with increasing vent uncertainty.

Vent uncertainty buffer distance	Evacuation clearance times (hours – 1 dp)					
	Free-flow vehicle capacity		2/3 Free-flow vehicle capacity		1/3 Free-flow vehicle capacity	
	Median	Max	Median	Max	Median	Max
0 km	36.8	40.3	37.2	42.5	38.5	49
1 km	37.0	40.3	37.5	42.5	39	49
3 km	37.3	40.9	38.0	43.4	40	50.8
5 km	37.6	41.3	38.4	44.0	40.9	52.1
7 km	37.9	41.3	38.9	44.0	41.8	52.1
10 km	38.4	42.4	39.7	45.7	43.4	55.4

5.3. Limitations to the AVF application

5.3.1. Data limitations

The implementation of the model for the AVF requires many assumptions to be made, given the limited datasets available. Several key assumptions and limitations are detailed below.

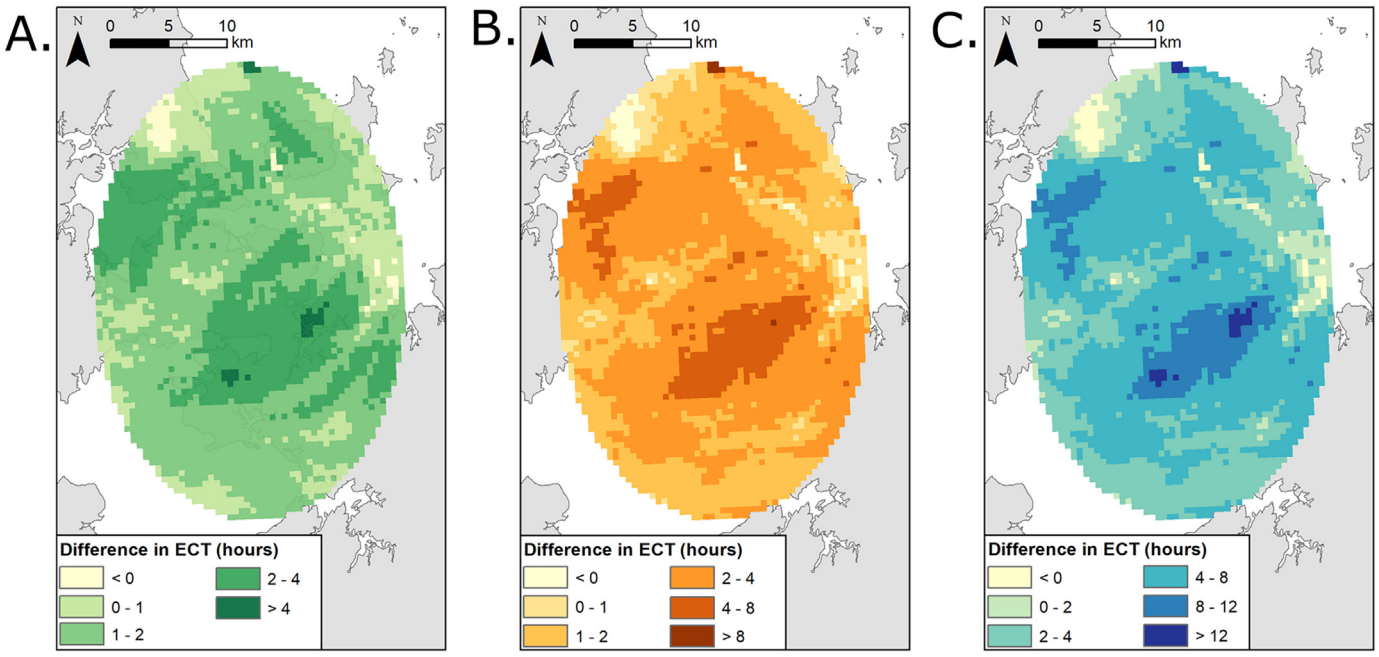

Fig. 15. Difference in evacuation clearance in hours for clearing a combined evacuation zone with 0 km and 10 km vent uncertainty for an eruption from any given vent within the AVF for (A) Free-flow capacity, (B) 2/3 Free-flow capacity and (C) 1/3 free-flow capacity for private owned vehicles.

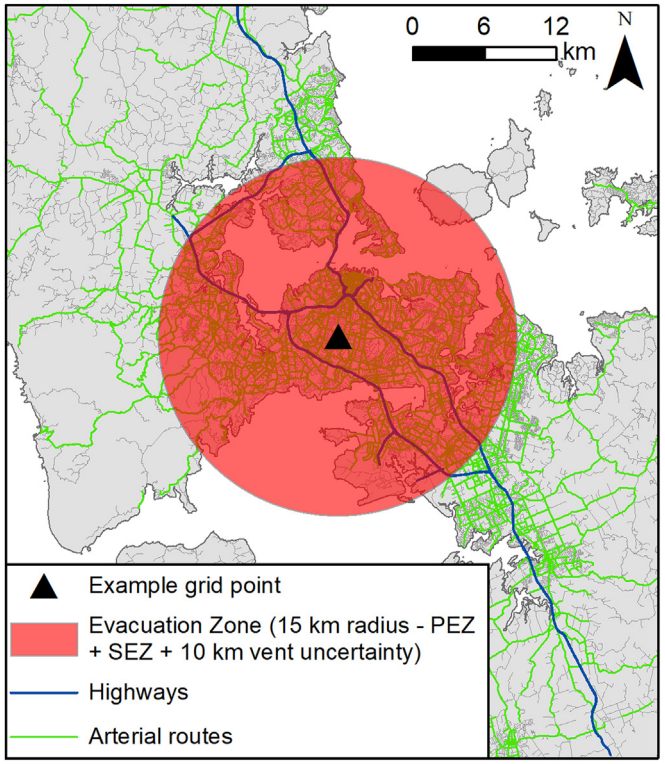

Fig. 16. Example of a central located vent with a 15 km radial evacuation zone with limited egress routes to egress routes only to the north-northwest and south.

When assessing the population exposure and subsequent evacuation clearance times, transient populations such as tourists and business travellers are not considered. Transient population data is not captured in the census dataset nor spatially well understood across Auckland. This population group can be difficult to convey evacuation notices to; a lack of regional hazard knowledge as well as language and cultural barriers have been noted as issues (Wright et al., 2014). However, with an increase in use of technology and social media to notify the public, the delay in notification of such transient populations could be minimal. Drabek (1999) found that people staying in hotels/motels are often notified by staff, potentially even at a faster rate than local residents. Additionally, transient populations will typically either have one private-use vehicle or evacuate via tour buses, which would likely add minimal vehicles to the departing traffic volume (Hobeika et al., 1994; Lindell and Prater, 2007).

The assessment of preparation (t_P) and travel (t_T) phases requires making assumptions about how people will behave following receiving the call to evacuate. We assessed population exposure based on assumed primary residence as recorded in the 2018 census, the same approach used by Blake et al. (2017) to assess population displacement. In other words, we assumed everyone would evacuate from home. While this is considered appropriate for events which provide some warning such as is expected for the AVF, this may not be appropriate for a rapid onset volcanic sequence or other hazards such as tsunami (in other words, people might need to evacuate from work or school in those scenarios). In addition, while the "from-work" evacuation preparation phase was factored into phase 3 (t_P) of the evacuation clearance time model, people returning home from work would put additional vehicles on the transportation network and/or require public transport support, which was not considered as part of this analysis.

We also made use of the responses from the self-reporting 2015 survey about peoples' preparedness for an AVF eruption (Coomer et al., 2015), especially when estimating evacuation order compliance and whether a household would evacuate together, which inform the preparation time (t_P). There are 21,000 people registered to receive such surveys from Auckland Council, but only 27% responded. This indicates the results could be potentially biased to those interested in the AVF and may not reflect the general consensus of Auckland. Additionally, participants may not be representative of all Aucklanders.

5.3.2. Model limitations

There are several factors not included in our model when considering the evacuation clearance time. These include phased and self-evacuations (Deligne et al., 2017), the direction evacuees go as they

leave the evacuation zone, and the time for vehicles to navigate to the egress route.

It is likely that a phased evacuation will be used during an AVF crisis (Wild et al., 2019a). To model this, output from this analysis could be disaggregated to consider first the PEZ clearance time, followed then by SEZ clearance time as the zones change while the event develops, as demonstrated in Deligne et al. (2017). However, the final evacuation zone (PEZ plus SEZ) could end up being smaller than the initial PEZ as the vent uncertainty area will reduce as the crisis develops (as demonstrated in Deligne et al., 2017), meaning that such a plan cannot be divorced from a strategy of early mass evacuation. In our study, we gave no consideration to those unable to self-evacuate, e.g. people in hospitals, rest-homes and prisons. These locations are likely to have longer evacuation clearance times, given the added logistics required. However, strategies for evacuating these types of locations are different and their evacuation will ideally commence earlier than that of the general public (Wild et al., 2019a).

There are few data available on the preferred direction in which people will evacuate, however for most vent locations there are alternate routes to move north or south. Due to this, for the purposes of this model, vehicles are equally split between all the available egress routes. As noted previously, there could be vent locations where only evacuations south are desirable, which will increase the traffic load and congestion on those egress routes. Additionally, background traffic is not included in this analysis as it is assumed there will be sufficient forewarning for traffic management to be put in place (Lindell and Prater, 2007).

The time for vehicles to navigate to the egress route is treated as negligible. This is because the travel distance is relatively short and it is assumed individuals will take the routes they know, including the small residential roads to reach the main arterials and highways to depart the evacuation zone. Through this approach the model assumes the bottleneck occurs at the roads that cross the evacuation zone boundary and makes the conservative assumption that all vehicles are crossing at the same time to inform the evacuation travel time. In reality this is not likely: the individual time delay in pre-travel activities will likely mean each household will depart at different times. Additionally, this modelling does not capture elements such as accidents blocking egress routes and weather effects that impact on the evacuation (Lindell and Prater, 2007).

6. Summary and conclusions

We have developed a volcanic crisis evacuation-support model and illustrated how it can be applied to an Auckland Volcanic Field (AVF) eruption. We provide an estimate of the total number of people that would likely need to be evacuated during a future AVF crisis, and examine how this number varies across Auckland. Furthermore, we provide an estimate of the number of people likely requiring public transport support to evacuate, and again show how this number varies spatially across the region. Finally, we provide the most complete treatment to date of evacuation clearance times for Auckland during an AVF crisis. Evacuation clearance times consider four phases: 1) the time taken to decide to call an evacuation; 2) the public notification time; 3) the evacuees' time to prepare; and 4) evacuees' travel time beyond the evacuation zone. The first three phases are all pre-travel and are informed by analogous hazards as there is limited published information from volcanic crises.

Key conclusions of our application to the AVF are:

- The median and maximum population within a 5 km evacuation zone (i.e. PEZ + SEZ, no vent uncertainty) are ~130,000 and 320,000, respectively, for considered vent locations across the AVF.
- When vent uncertainty is added to the 5 km evacuation zone, the maximum exposed population increases to ~375,000 for a 1 km buffer, and up to 1.1 million for a 10 km buffer.
- A vent located in or around the CBD impacts the greatest number of people, and will require the most public transport support, as these areas are both densely populated and have the lowest vehicle ownership rates.
- The pre-travel decision time (t_D) is completed within 36 h with over 80% confidence.
- The total evacuation clearance time ranges between 37 and 40 h for the 5 km evacuation zone with no vent uncertainty buffer applied, when considering free-flowing road carrying capacity. This increases to a maximum of 49 h when vehicle carrying capacity is reduced to a third.
- The worst-case clearance time found was when a vent uncertainty of 10 km is applied and the vehicle carrying capacity is reduced to a third, resulting in a clearance time of ~55 h.
- The areas with the longest clearance times are those residential suburbs with relatively limited egress routes.
- The total pre-travel time is strongly influenced by the time taken to decide to call an evacuation. The travel time (t_T) is dependent on the number of people and vehicles, the number of egress routes and their carrying capacity beyond the evacuation zone, and the level of congestion on the network.
- Weighting the vent likelihood based on past AVF spatial vent models had negligible effect on evacuation clearance times.

Although our application assessed population exposure and evacuation times for all possible vents across Auckland, it would also be very easy to provide these outputs for a specific vent location or a more constrained area within the AVF. The model can also be updated and refined as more data on population exposure and the times for each evacuation phase become available. In addition, this approach could also be applied to assess the population exposure and subsequent evacuation clearance time for other hazards, and for other regions. While more advanced models exist for assessing travel times, our approach does provide a very computationally efficient and robust method, needing fewer uncertain inputs than are required for more advanced agent-based modelling and transportation models.

Funding

The Determining Volcanic Risk in Auckland (DEVORA) research programme and the New Zealand Earthquake Commission (EQC) provided funding for this project. MSB was supported by the Resilience to Nature's Challenges Volcano Programme, Grant GNS-RNC047.

Declaration of Competing Interest

The authors declare that they have no known competing financial interests or personal relationships that could have appeared to influence the work reported in this paper.

Acknowledgements

The authors would like to thank Seosamh Costello for providing feedback on part of the model concept. We also greatly appreciate the thoughtful reviews of two anonymous reviewers, and the supportive editorial work by José Luis Macias.

Appendix A. Supplementary data

Supplementary data to this article can be found online at https://doi.org/10.1016/j.jvolgeores.2021.107282.

References

Afzal, M., Ranjitkar, P., Costello, S.B., 2019. Auckland evacuation model: development and calibration. Presented at the Engineering NZ Transportation Group 2019 Conference. Wellington, New Zealand.

Allen, S.R., Smith, I.E.M., 1994. Eruption styles and volcanic hazard in the Auckland Volcanic Field, New Zealand. Geosci. Rep. Shizuoka Univ. 20, 5–14.

Allen, S.R., Bryner, V.F., Smith, I.E.M., Ballance, P.F., 1996. Facies analysis of pyroclastic deposits within basaltic tuff-rings of the Auckland volcanic field, New Zealand. N. Z. J. Geol. Geophys. 39, 309–327.

Ang, P.S., Bebbington, M.S., Lindsay, J.M., Jenkins, S.F., 2020. From eruption scenarios to probabilistic volcanic hazard analysis: an example of the Auckland Volcanic Field, New Zealand. J. Volcanol. Geotherm. Res. https://doi.org/10.1016/j.jvolgeores.2020.106871.

Auckland Council, 2014. Auckland Evacuation Plan. http://www.aucklandcivildefence.org.nz/media/48200/BC3598-Auckland-Evacuation-Plan_WEB-spreads-.pdf (Accessed 06.02.16).

Auckland Council, 2015. Auckland Volcanic Field Contingency Plan. http://www.aucklandcivildefence.org.nz/media/48896/2015-03-27-Auckland-Volcanic-Field-Contingency-Plan-Version-2-.pdf (Accessed 06.02.16).

Auckland Region CDEM Group, 2008. Final Exercise Report. Exercise Ruaumoko '08. Ministry of Civil Defence & Emergency Management, Auckland, New Zealand.

Auckland Transport, 2020. Auckland Transport Open GIS Data: Average Daily Traffic Counts [WWW Document]. Average Daily Traffic Counts https://data-atgis.opendata.arcgis.com/datasets/average-daily-traffic-counts/data?geometry=173.846%2C-37.079%2C176.153%2C-36.695 (Accessed 11.5.20).

Auker, M.R., Sparks, R.S.J., Siebert, L., Crosweller, H.S., Ewert, J., 2013. A statistical analysis of the global historical volcanic fatalities record. J. Appl. Volcanol. 2, 1–24. https://doi.org/10.1186/2191-5040-2-2.

Baker, E.J., 1991. Hurricane evacuation behavior. Int. J. Mass Emerg. Disasters 9, 287–310.

Barberi, F., Carapezza, M., 1996. The problem of volcanic unrest: the Campi Flegrei case history. Monitoring and Mitigation of Volcano Hazards. Springer, pp. 771–786.

Barclay, J., Few, R., Armijos, M.T., Phillips, J.C., Pyle, D.M., Hicks, A., Brown, S.K., Robertson, R.E.A., 2019. Livelihoods, wellbeing and the risk to life during volcanic eruptions. Front. Earth Sci. 7, 1–15. https://doi.org/10.3389/feart.2019.00205.

Bautista, C.B., 1996. The Mount Pinatubo Disaster and the People of Central Luzon, in: Publication Title: Fire and Mud: Eruptions and Lahars of Mount Pinatubo, Philippines. University of Washington Press, Quezon City and Seattle, Seattle.

Bay of Plenty Emergency Management Group, 2021. Emergency Status Page: National Warning: Tsunami Threat – Immediate Evacuation Required for some Areas [WWW Document]. URL. http://www.bopcivildefence.govt.nz/starstaremergency-status-pagestarstar/.

Bebbington, M.S., 2013. Assessing spatio-temporal eruption forecasts in a monogenetic volcanic field. J. Volcanol. Geotherm. Res. 252, 14–28. https://doi.org/10.1016/j.jvolgeores.2012.11.010.

Bebbington, M.S., 2015. Spatio-volumetric hazard estimation in the Auckland volcanic field. Bull. Volcanol. 77. https://doi.org/10.1007/s00445-015-0921-3.

Bebbington, M.S., Cronin, S.J., 2011. Spatio-temporal hazard estimation in the Auckland Volcanic Field, New Zealand, with a new event-order model. Bull. Volcanol. 73, 55–72. https://doi.org/10.1007/s00445-010-0403-6.

Bebbington, M.S., Zitikis, R., 2016. Dynamic uncertainty in cost-benefit analysis of evacuation prior to a volcanic eruption. Math. Geosci. https://doi.org/10.1007/s11004-015-9615-9.

Belousov, A., Voight, B., Belousova, M., 2007. Directed blasts and blast-generated pyroclastic density currents: a comparison of the Bezymianny 1956, Mount St Helens 1980, and Soufrière Hills, Montserrat 1997 eruptions and deposits. Bull. Volcanol. 69, 701–740. https://doi.org/10.1007/s00445-006-0109-y.

Bird, D.K., Gísladóttir, G., 2018. Responding to volcanic eruptions in Iceland: from the small to the catastrophic. Palgrave Commun. 4, 151. https://doi.org/10.1057/s41599-018-0205-6.

Bird, D.K., Gisladottir, G., Dominey-Howes, D., 2009. Resident perception of volcanic hazards and evacuation procedures. Nat. Hazards Earth Syst. Sci. 9, 251–266. https://doi.org/10.5194/nhess-9-251-2009.

Blake, S., 2006. Lead Times and Precursors of Eruptions in the Auckland Volcanic Field, New Zealand: Indications from Historical Analogues and Theoretical Modelling. GNS Science, Lower Hutt, N.Z.

Blake, D.M., Deligne, N.I., Wilson, T.M., Lindsay, J.M., Woods, R., 2017. Investigating the consequences of urban volcanism using a scenario approach II: Insights into transportation network damage and functionality. J. Volcanol. Geotherm. Res. 340, 92–116. https://doi.org/10.1016/j.jvolgeores.2017.04.010.

Blendon, R.J., Benson, J.M., DesRoche, C.M., Lyon-Daniel, K., Mitchell, E.W., Pollard, W.E., 2007. The Public's Preparedness for Hurricanes in Four Affected Regions. Public Health Reports 122, 167–176. https://doi.org/10.1177/003335490712200206.

Blong, R.J., 1984. Volcanic Hazards. A Sourcebook on the Effects of Eruptions.

Brand, B.D., Gravley, D.M., Clarke, A.B., Lindsay, J.M., Bloomberg, S.H., Agustin-Flores, J., Németh, K., 2014. A combined field and numerical approach to understanding dilute pyroclastic density current dynamics and hazard potential: Auckland Volcanic Field, New Zealand. J. Volcanol. Geotherm. Res. 276, 215–232. https://doi.org/10.1016/j.jvolgeores.2014.01.008.

Brenna, M., Cronin, S.J., Smith, I.E.M., Tollan, P.M.E., Scott, J.M., Prior, D.J., Bambery, K., Ukstins, I.A., 2018. Olivine xenocryst diffusion reveals rapid monogenetic basaltic magma ascent following complex storage at Pupuke Maar, Auckland Volcanic Field, New Zealand. Earth Planet. Sci. Lett. 499, 13–22. https://doi.org/10.1016/j.epsl.2018.07.015.

Bretton, R.J., Gottsmann, J., Aspinall, W.P., Christie, R., 2015. Implications of legal scrutiny processes (including the L'Aquila trial and other recent court cases) for future volcanic risk governance. J. Appl. Volcanol. 4, 2–24. https://doi.org/10.1186/s13617-015-0034-x.

Bretton, R., Gottsmann, J., Christie, R., 2017. The Role of Laws within the Governance of Volcanic Risks, in: Volcanic Unrest. Springer, Cham, pp. 23–34.

Brown, S.K., Auker, M.R., Sparks, R.S.J., 2015. Populations around Holocene volcanoes and development of a Population Exposure Index. Glob. Volcanic Haz. Risk, 223–232 https://doi.org/10.1017/CBO9781316276273.006.

Brown, S.K., Jenkins, S.F., Sparks, R.S.J., Odbert, H., Auker, M.R., 2017. Volcanic fatalities database: analysis of volcanic threat with distance and victim classification. J. Appl. Volcanol. 6 (1), 1–20. https://doi.org/10.1186/s13617-017-0067-4.

Brunsdon, D., Park, B., 2009. Lifeline vulnerability to volcanic eruption: learnings from a national simulation exercise. TCLEE 2009: Lifeline Earthquake Engineering in a Multihazard Environment, pp. 1–12.

Brunton, Colmar, 2020. Emergency Mobile Alert System: Follow-Up Survey for the Nationwide Test on Sunday 24 November 2019.

CDEM Act, 2002. Civil Defence Emergency Management Act. https://www.legislation.govt.nz/act/public/2002/0033/latest/whole.html (Accessed 5.13.21).

Charlton, D., Kilburn, C., Edwards, S., 2020. Volcanic unrest scenarios and impact assessment at Campi Flegrei caldera, Southern Italy. J. Appl. Volcanol. 9, 7. https://doi.org/10.1186/s13617-020-00097-x.

Chenet, M., Grancher, D., Redon, M., 2014. Main issues of an evacuation in case of volcanic crisis: social stakes in Guadeloupe (Lesser Antilles Arc). Nat. Hazards 73, 2127–2147. https://doi.org/10.1007/s11069-014-1184-6.

Chester, D.K., Degg, M., Duncan, A.M., Guest, J.E., 2000. The increasing exposure of cities to the effects of volcanic eruptions: a global survey. Environ. Hazards 2, 89–103. https://doi.org/10.3763/ehaz.2000.0214.

Chinander Dye, K., Eggers, J.P., Shapira, Z., 2014. Trade-offs in a tempest: stakeholder influence on hurricane evacuation decisions. Organ. Sci. 25, 1009–1025.

Clark, A.E., Hagelman, R.R., Dixon, R.W., 2020. Modeling a contraflow evacuation method for tropical cyclone evacuations in Nueces County, Texas. Nat. Hazards https://doi.org/10.1007/s11069-020-04101-w.

Cola, R.M., 1996. Responses of Pampanga Households to Lahar Warnings: Lessons from Two Villages in the Pasig-Potrero River Watershed, in: Fire and Mud: Eruptions and Lahars of Mount Pinatubo, Philippines. Philippine Institute of Volcanology and Seismology and University of Washington Press, Quezon City and Seattle.

Cole, J., Blumenthal, E., 2004. Evacuate: what an evacuation order given because of a pending volcanic eruption could mean to residents of Bay of Plenty. Tephra: Living with Volcanoes. Ministry of Civil Defense and Emergency Management, New Zealand, pp. 47–52.

Coomer, M.A., Bates, A., Keith, H., Lambie, E.S., Leonard, G., Maxwell, K., Potter, S.H., Wilson, T.M., GNS Science (N.Z.), 2015. DEVORA Volcanic Survey: People's Panel.

Cova, T.J., Church, R.L., 1997. Modelling community evacuation vulnerability using GIS. Int. J. Geogr. Inf. Sci. 11, 763–784. https://doi.org/10.1080/136588197242077.

COVID-19 Group, 2021. COVID-19 Alert System [WWW Document]. Unite Against COVID-19. https://covid19.govt.nz/alert-system/ (Accessed 3.16.21).

Cronin, S.J., 2008. The Auckland Volcanic Scientific Advisory Group during Exercise Ruaumoko: Observations and Recommendations. Civil Defence Emergency Management: Exercise Ruaumoko. Auckland Regional Council, Auckland.

Deligne, N.I., Blake, D.M., Davies, A.J., Grace, E.S., Hayes, J.L., Potter, S., Stewart, C., Wilson, G., Wilson, T.M., 2015. Economics of Resilient Infrastructure Auckland Volcanic Scenario.

Deligne, N.I., Fitzgerald, R.H., Blake, D.M., Davies, A.J., Hayes, J.L., Stewart, C., Wilson, G., Wilson, T.M., Castelino, R., Kennedy, B.M., Muspratt, S., Woods, R., 2017. Investigating the consequences of urban volcanism using a scenario approach I: Development and application of a hypothetical eruption in the Auckland Volcanic Field, New Zealand. J. Volcanol. Geotherm. Res. 336, 192–208. https://doi.org/10.1016/j.jvolgeores.2017.02.023.

Dow, K., Cutter, S.L., 1998. Crying wolf: repeat responses to hurricane evacuation orders. Coast. Manag. 26, 237–252. https://doi.org/10.1080/08920759809362356.

Dow, K., Cutter, S.L., 2002. Emerging hurricane evacuation issues: hurricane Floyd and South Carolina. Nat. Hazards Rev. 3, 12–18.

Doyle, E.E.H., Paton, D., Johnston, D.M., 2015. Enhancing scientific response in a crisis: evidence-based approaches from emergency management in New Zealand. J. Appl. Volcanol. 4, 1. https://doi.org/10.1186/s13617-014-0020-8.

Drabek, T.E., 1999. Disaster evacuation responses by tourists and other types of transients. Int. J. Public Adm. 22, 655–677. https://doi.org/10.1080/01900699908525400.

Elissondo, M., Baumann, V., Bonadonna, C., Pistolesi, M., Cioni, R., Bertagnini, A., Biass, S., Herrero, J.-C., Gonzalez, R., 2016. Chronology and impact of the 2011 Cordón Caulle eruption, Chile. Nat. Hazards Earth Syst. Sci. 16, 675–704. https://doi.org/10.5194/nhess-16-675-2016.

Floret, N., Viel, J.-F., Mauny, F., Hoen, B., Piarroux, R., 2006. Negligible Risk for Epidemics after Geophysical disasters. Emerg. Infect. Dis. 12, 543–548. https://doi.org/10.3201/eid1204.051569.

Garber, N.J., Hoel, L.A., 2010. Traffic & Highway Engineering-SI Version. 4th ed. Cengage Learning SI ed.

Green, D., Lewis, K., Head, A., Ward, J., Munro, C., 2020. Guide to Traffic Management Part 3: Transport Study and Analysis Methods (No. AGTM03-20). AustRoads.

Guðmundsson, M., Gylfason, Á., 2005. Hættumat vegan eldgosa og hlaupa frá vestanverðum Mýrdalsjökli og Eyjafjallajökli. Ríkislögreglustjórinn, Reykjavík 210.

Hayes, J.L., Tsang, S.W., Fitzgerald, R.H., Blake, D.M., Deligne, N.I., Doherty, A., Hopkins, J.L., Hurst, A.W., Le Corvec, N., Leonard, G.S., Lindsay, J.M., Miller, C.A., Nemeth, K., Smid, E., White, J.D.L., Wilson, T.M., 2018. The DEVORA Scenarios: Multi-hazard Eruption Scenarios for the Auckland Volcanic Field. Lower Hutt (NZ) https://doi.org/10.21420/G20652.

Hayes, J.L., Wilson, T.M., Deligne, N.I., Lindsay, J.M., Leonard, G.S., Tsang, S.W.R., Fitzgerald, R.H., 2019. Developing a suite of multi-hazard volcanic eruption scenarios using an interdisciplinary approach. J. Volcanol. Geotherm. Res., 106763 https://doi.org/10.1016/j.jvolgeores.2019.106763.

Hobeika, A.G., Kim, S., Beckwith, R.E., 1994. A decision support system for developing evacuation plans around nuclear power stations. Interfaces 24, 22–35.

Hong, L., Frias-Martinez, V., 2020. Modeling and predicting evacuation flows during hurricane Irma. EPJ Data Sci. 9, 29. https://doi.org/10.1140/epjds/s13688-020-00247-6.

Hopkins, J.L., Wilson, C.J.N., Millet, M., Leonard, G.S., Timm, C., Mcgee, L.E., Smith, I.E.M., Smith, E.G.C., 2017. Multi-criteria Correlation of Tephra Deposits to Source Centres Applied in the Auckland Volcanic Field, New Zealand. https://doi.org/10.1007/s00445-017-1131-y.

Hopkins, J.L., Smid, E.R., Eccles, J.D., Hayes, J.L., Hayward, B.W., McGee, L.E., van Wijk, K., Wilson, T.M., Cronin, S.J., Leonard, G.S., Lindsay, J.M., Németh, K., Smith, I.E.M., 2020. Auckland Volcanic Field magmatism, volcanism, and hazard: a review. N. Z. J. Geol. Geophys., 1–22 https://doi.org/10.1080/00288306.2020.1736102.

Horrocks, J., 2008. Learning from Exercise Ruaumoko, Exercise Ruaumoko 2008. Ministry of Civil Defence and Emergency Management, New Zealand.

Horspool, N.A., Savage, M.K., Bannister, S., 2006. Implications for intraplate volcanism and back-arc deformation in northwestern New Zealand, from joint inversion of receiver functions and surface waves. Geophys. J. Int. 166, 1466–1483. https://doi.org/10.1111/j.1365-246X.2006.03016.x.

Jumadi Heppenstall, A.J., Malleson, N.S., Carver, S.J., Quincey, D.J., Manville, V.R., 2018. Modelling individual evacuation decisions during natural disasters: a case study of volcanic crisis in Merapi, Indonesia. Geosciences (Switzerland) 8, 1–30. https://doi.org/10.3390/geosciences8060196.

Kang, J.E., Lindell, M.K., Prater, C.S., 2007. Hurricane evacuation expectations and actual behavior in Hurricane Lili. J. Appl. Soc. Pyschol. 37, 887–903. https://doi.org/10.1111/j.1559-1816.2007.00191.x.

Kereszturi, G., Németh, K., Cronin, S.J., Agustín-Flores, J., Smith, I.E.M., Lindsay, J., 2013. A model for calculating eruptive volumes for monogenetic volcanoes — Implication for the Quaternary Auckland Volcanic Field, New Zealand. J. Volcanol. Geotherm. Res. 266, 16–33. https://doi.org/10.1016/j.jvolgeores.2013.09.003.

Kereszturi, G., Németh, K., Cronin, S.J., Procter, J., Agustín-Flores, J., 2014. Influences on the variability of eruption sequences and style transitions in the Auckland Volcanic Field, New Zealand. J. Volcanol. Geotherm. Res. 286, 101–115. https://doi.org/10.1016/j.jvolgeores.2014.09.002.

Lane, L.R., Tobin, G.A., Whiteford, L.M., 2003. Volcanic hazard or economic destitution: hard choices in Baños, Ecuador. Environ. Hazards 5, 23–34. https://doi.org/10.1016/j.hazards.2004.01.001.

Lavigne, F., Morin, J., Mei, E.T.W., Calder, E.S., Usamah, M., Nugroho, U., 2018. Mapping hazard zones, rapid warning communication and understanding communities: primary ways to mitigate pyroclastic flow hazard. In: Fearnley, C.J., Bird, D.K., Haynes, K., McGuire, W.J., Jolly, G. (Eds.), Observing the Volcano World: Volcano Crisis Communication. Springer International Publishing, Cham, pp. 107–119 https://doi.org/10.1007/11157_2016_34.

Leonard, G.S., Calvert, A.T., Hopkins, J.L., Wilson, C.J.N., Smid, E.R., Lindsay, J.M., Champion, D.E., 2017. High-precision 40 Ar/39 Ar dating of Quaternary basalts from Auckland Volcanic Field, New Zealand, with implications for eruption rates and paleomagnetic correlations. J. Volcanol. Geotherm. Res. 343, 60–74. https://doi.org/10.1016/j.jvolgeores.2017.05.033.

Lindell, M.K., 2008. EMBLEM2: an empirically based large scale evacuation time estimate model. Transp. Res. A Policy Pract. 42, 140–154. https://doi.org/10.1016/j.tra.2007.06.014.

Lindell, M.K., Perry, R.W., 1992. Behavioral foundations of community emergency planning. Behavioral Foundations of Community Emergency Planning. Hemisphere Publishing Corp, Washington, DC, US.

Lindell, M., Perry, R., 2004. Communicating Environmental Risk in Multiethnic Communities. Sage Publication.

Lindell, M.K., Perry, R.W., 2012. The Protective Action Decision Model: Theoretical Modifications and Additional Evidence. p. 17.

Lindell, M.K., Prater, C.S., 2007. Critical behavioral assumptions in evacuation time estimate analysis for private vehicles: examples from Hurricane Research and Planning. J. Urban Plan. Dev. 133, 18–29. https://doi.org/10.1061/(ASCE)0733-9488(2007)133:1(18).

Lindell, M.K., Prater, C.S., Sanderson, W.G., Lee, H.M., Yang, Z., Mohite, A., Hwang, S.N., 2001. Texas Gulf Coast residents' Expectations and Intentions Regarding Hurricane Evacuation. Hazard Reduction & Recovery Center, Texas A & M University.

Lindell, M.K., Prater, C.S., Perry, R.W., Wu, J.Y., 2002. EMBLEM: An Empirically Based Large-scale Evacuation Time Estimate Model. Report. Hazard Reduction & Recovery Center, Texas A & M University, College Station, Texas.

Lindell, M.K., Lu, J.-C., Prater, C.S., 2005. Household decision making and evacuation in response to Hurricane Lili. Nat. Hazards Rev. 6, 171–179. https://doi.org/10.1061/(ASCE)1527-6988(2005)6:4(171).

Lindell, M.K., Prater, C.S., Peacock, W.G., 2007. Organizational communication and decision making for Hurricane emergencies. Nat. Hazards Rev. 8, 50–60. https://doi.org/10.1061/(ASCE)1527-6988(2007)8:3(50).

Lindell, M.K., Sorensen, J.H., Baker, E.J., Lehman, W.P., 2020. Community response to hurricane threat: estimates of household evacuation preparation time distributions. Transp. Res. Part D: Transp. Environ. 85, 102457. https://doi.org/10.1016/j.trd.2020.102457.

Lindsay, J., Marzocchi, W., Jolly, G.E., Constantinescu, R., Selva, J., Sandri, L., 2010. Towards real-time eruption forecasting in the Auckland Volcanic Field: application of BET_EF during the New Zealand National Disaster Exercise "Ruaumoko". Bull. Volcanol. 72, 185–204. https://doi.org/10.1007/s00445-009-0311-9.

Lindsay, J.M., Leonard, G.S., Smid, E.R., Hayward, B.W., 2011. Age of the Auckland Volcanic Field: a review of existing data. N. Z. J. Geol. Geophys. 54, 379–401. https://doi.org/10.1080/00288306.2011.595805.

Magill, C.R., Blong, R.J., 2005. Volcanic risk ranking for Auckland, New Zealand. II: hazard consequences and risk calculation. Bull. Volcanol. 67, 340–349. https://doi.org/10.1007/s00445-004-0375-5.

Magill, C.R., McAneney, K.J., Smith, I.E., 2005. Probabilistic assessment of vent locations for the next Auckland volcanic field event. Math. Geol. 37, 227–242. https://doi.org/10.1007/s11004-005-1556-2.

Marrero, J.M., García, A., Llinares, A., Rodríguez-Losada, J.A., Ortiz, R., 2010. The Variable Scale Evacuation Model (VSEM): a new tool for simulating massive evacuation processes during volcanic crises. Nat. Hazards Earth Syst. Sci. 10, 747–760. https://doi.org/10.5194/nhess-10-747-2010.

Marzocchi, W., 2012. Putting science on trial. Phys. World 25, 17.

Marzocchi, W., Woo, G., 2007. Probabilistic eruption forecasting and the call for an evacuation. Geophys. Res. Lett. 34, 2–5. https://doi.org/10.1029/2007GL031922.

Marzocchi, W., Woo, G., 2009. Principles of volcanic risk metrics: Theory and the case study of Mount Vesuvius and Campi Flegrei, Italy. J. Geophys. Res. Solid Earth 114.

Marzocchi, W., Sandri, L., Selva, J., 2008. BET_EF: a probabilistic tool for long- and short-term eruption forecasting. Bull. Volcanol. 70, 623–632. https://doi.org/10.1007/s00445-007-0157-y.

MCDEM, 2015. The Guide to the National Civil Defence Emergency Management Plan 2015. Ministry of Civil Defence & Emergency, Wellington.

Mei, E.T.W., Lavigne, F., 2012. Influence of the institutional and socio-economic context for responding to disasters: case study of the 1994 and 2006 eruptions of the Merapi Volcano, Indonesia. Geol. Soc. Lond., Spec. Publ. 361, 171–186. https://doi.org/10.1144/SP361.14.

Moriarty, K.D., Ni, D., Collura, J., 2007. Modeling traffic flow under emergency evacuation situations: Current practice and future directions. 86th Transportation Research Board Annual Meeting. Washington DC.

Morrissey, M., Zimanowski, B., Wohletz, K., Buettner, R., 2000. Phreatomagmatic fragmentation. In: Sigurdsson, H., Houghton, B., McNutt, S.R., Rymer, H., Stix, J. (Eds.), Encyclopedia of Volcanoes. Academic Press, pp. 431–445.

Na, H.S., Banerjee, A., 2019. Agent-based discrete-event simulation model for no-notice natural disaster evacuation planning. Comput. Ind. Eng. 129, 44–55. https://doi.org/10.1016/j.cie.2019.01.022.

Needham, A.J., Lindsay, J.M., Smith, I.E.M., Augustinus, P., Shane, P.A., 2011. Sequential eruption of alkaline and sub-alkaline magmas from a small monogenetic volcano in the Auckland Volcanic Field, New Zealand. J. Volcanol. Geotherm. Res. 201, 126–142. https://doi.org/10.1016/j.jvolgeores.2010.07.017.

NEMA, 2020. New Zealand Volcanic Science Advisory Panel (NZVSAP) Terms of Reference. https://www.civildefence.govt.nz/assets/Uploads/publications/nzvsap-tor-sep-2020.pdf.

NEMA, 2021. National Warning: Tsunami Threat to Land and Marine Areas. Scoop. https://www.scoop.co.nz/stories/AK2103/S00106/national-warning-tsunami-threat-to-land-and-marine-areas.htm (Accessed 03.12.21).

New Zealand Transport Agency, 2013. One Network Road Classification. Wellington, New Zealand.

Newhall, C.G., Punongbayan, A.S., 1996. Fire and Mud, Eruptions and Lahars of Mount Pinatubo, Philipines. , p. 2 https://doi.org/10.2307/3673980.

Newhall, C., Ii, J.W.H., Stauffer, P.H., 1998. U. S. Geological Survey — Reducing the Risk from Volcano Hazards The Cataclysmic 1991 Eruption of Mount Pinatubo, Philippines.

Papale, P., 2017. Rational Volcanic Hazard Forecasts and the Use of Volcanic Alert Levels. https://doi.org/10.1186/s13617-017-0064-7.

Perry, S.D., 2007. Tsunami Warning Dissemination in Mauritius. J. Appl. Commun. Res. 35, 399–417. https://doi.org/10.1080/00909880701611060.

Potter, S.H., Jolly, G.E., Neall, V.E., Johnston, D.M., Scott, B.J., 2014. Communicating the status of volcanic activity: revising New Zealand's volcanic alert level system. J. Appl. Volcanol. 3 (1), 1–13. https://doi.org/10.1186/s13617-014-0013-7.

Quarantelli, E.L., 1980. Evacuation Behavior and Problems: Findings and Implications from the Research Literature. OHIO State University Columbus Disaster Research Center.

Rogers, G.O., Sorensen, J.H., 1988. Diffusion of emergency warnings. Environ. Profess. 10, 185–198.

Runge, M.G., Bebbington, M.S., Cronin, S.J., Lindsay, J.M., Moufti, M.R., 2015. Sensitivity to volcanic field boundary. J. Appl. Volcanol. 4, 22. https://doi.org/10.1186/s13617-015-0040-z.

Sakamoto, M., Sasaki, D., Ono, Y., Makino, Y., Kodama, E.N., 2020. Implementation of evacuation measures during natural disasters under conditions of the novel coronavirus (COVID-19) pandemic based on a review of previous responses to complex disasters in Japan. Prog. Disast. Sci. 8, 100127. https://doi.org/10.1016/j.pdisas.2020.100127.

Sandri, L., Jolly, G.E., Lindsay, J., Howe, T., Marzocchi, W., 2012. Combining long-and short-term probabilistic volcanic hazard assessment with cost-benefit analysis to support decision making in a volcanic crisis from the Auckland Volcanic Field, New Zealand. Bull. Volcanol. 74, 705–723.

Selva, J., Marzocchi, W., Papale, P., Sandri, L., 2012. Operational eruption forecasting at high-risk volcanoes: the case of Campi Flegrei, Naples. J. Appl. Volcanol. 1, 1–14. https://doi.org/10.1186/2191-5040-1-5.

Sherburn, S., Scott, B., Olsen, J., Miller, C., 2007. Monitoring seismic precursors to an eruption from the Auckland Volcanic Field, New Zealand. N. Z. J. Geol. Geophys. 50, 1–11. https://doi.org/10.1080/00288300709509814.

Small, C., Naumann, T., 2001. The global distribution of human population and recent volcanism. Environ. Hazards 3, 93–109. https://doi.org/10.1016/S1464-2867(02)00002-5.

Smid, E., Lindsay, J., Jolly, G., Fields, B., 2009. A Review of Statistical Methods Used to Assess Probabilistic Hazard in Monogenetic Basaltic Fields a Review of Statistical Methods Used to Assess Probabilistic Hazard in Monogenetic.

Solutions Pacific LLC, 2018. State of Hawaii Hurricane Behavioral Survey. https://dod.hawaii.gov/hiema/files/2020/02/DEC_2018-Hurricane-Behavioral-Survey.pdf.

Sorensen, J.H., Lindell, M.K., Baker, E.J., Lehman, W.P., 2020. Community response to Hurricane threat: estimates of warning issuance time distributions. Weather Clim. Soc. 12, 837–846. https://doi.org/10.1175/WCAS-D-20-0031.1.

Statistics New Zealand, 2018. Auckland Region [WWW Document]. https://www.stats.govt.nz/tools/2018-census-place-summaries/auckland-region.

Statistics New Zealand, 2019a. Regional Gross Domestic Product: Year Ended March 2018 [WWW Document]. https://www.stats.govt.nz/information-releases/regional-gross-domestic-product-year-ended-march-2018.
Statistics New Zealand, 2019b. Territorial Authority Local Board 2018 (Generalised) [WWW Document]. https://datafinder.stats.govt.nz/layer/103910-territorial-authority-local-board-2018-generalised/.
Tayag, J., Insauriga, S., Ringor, A., Belo, M., 1996. People's response to eruption warning: The Pinatubo experience, 1991–92. Fire and Mud. Eruptions and Lahars of Mount Pinatubo. University of Washington Press, Philippines.
Tierney, K.J., Lindell, M.K., Perry, R.W., 2002. Facing the unexpected: disaster preparedness and response in the United States. Disast. Prevent. Manag.: Int. J. 11 (3), 222. https://doi.org/10.1108/dpm.2002.11.3.222.1.
Tobin, G.A., Whiteford, L.M., 2002. Community Resilience and Volcano Hazard: the Eruption of Tungurahua and Evacuation of the Faldas in Ecuador. Disasters 26, 28–48. https://doi.org/10.1111/1467-7717.00189.
Tomsen, E., Lindsay, J.M., Gahegan, M., Wilson, T.M., Blake, D.M., 2014. Evacuation planning in the Auckland Volcanic Field, New Zealand: a spatio-temporal approach for emergency management and transportation network decisions. J. Appl. Volcanol. 3, 1–22. https://doi.org/10.1186/2191-5040-3-6.
Transportation Research Board (Ed.), 2016. Publication Title: Highway Capacity Manual - A Guide for Multimodal Mobility Analysis (6th Edition), 6th ed. Transportation Research Board, Washington D.C.
Trevett, C., 2020. Covid 19 Coronavirus: PM Jacinda Ardern and the Six Hours Back into Lockdown. New Zealand Herald.
Urbanik, T., Desrosiers, A., Lindell, M., Schuller, C., 1980. Analysis of Techniques for Estimating Evacuation Times for Emergency Planning Zones (No. (No. NUREG/CR–1745)). Texas Transportation Institute (United States).
Wild, A.J., Lindsay, J.M., Costello, S.B., Deligne, N.I., Doherty, A., Leonard, G.S., Maxwell, K., Rollin, J., Wilson, T.M., 2019a. Auckland Volcanic Field eruption crisis management decision-making pilot workshop (No. GNS Science report; 2019/70), 2019/70. GNS Science. Lower Hutt (NZ) https://doi.org/10.21420/[V1B6-NC4].
Wild, A.J., Wilson, T.M., Bebbington, M.S., Cole, J.W., Craig, H.M., 2019b. Probabilistic volcanic impact assessment and cost-benefit analysis on network infrastructure for secondary evacuation of farm livestock: a case study from the dairy industry, Taranaki, New Zealand. J. Volcanol. Geotherm. Res. 387, 106670. https://doi.org/10.1016/j.jvolgeores.2019.106670.
Wilson, T.M., Cole, J.W., Johnston, D.M., Cronin, S.J., Stewart, C., Dantas, A., 2012. Short- and long-term evacuation of people and livestock during a volcanic crisis: lessons from the 1991 eruption of Volcan Hudson, Chile. J. Appl. Volcanol. 1, 1–11. https://doi.org/10.1186/2191-5040-1-2.
Wohletz, K.H., Sheridan, M.F., 1979. A Model of Pyroclastic Surge 177–194. https://doi.org/10.1130/spe180-p177.
Wolshon, B., Urbina, E., Wilmot, C., Levitan, M., 2005. Review of policies and practices for Hurricane evacuation. I: transportation planning, preparedness, and response. Nat. Hazards Rev. 6, 129–142. https://doi.org/10.1061/(ASCE)1527-6988(2005)6:3(129).
Woo, G., 2008. Probabilistic criteria for volcano evacuation decisions. Nat. Hazards 45, 87–97. https://doi.org/10.1007/s11069-007-9171-9.
Wright, K., Beatson, A., Coomer, M.A., Freire, D., Leonard, G., Morris, B., O'Sullivan, R., GNS Science (N.Z.), 2014. Public Alerting Options Assessment: 2014 Update.
Wu, H.-C., Lindell, M.K., Prater, C.S., 2012. Logistics of hurricane evacuation in Hurricanes Katrina and Rita. Transport. Res. F: Traffic Psychol. Behav. 15, 445–461. https://doi.org/10.1016/j.trf.2012.03.005.
Yin, D., Wang, S., Ouyang, Y., 2020. ViCTS: a novel network partition algorithm for scalable agent-based modeling of mass evacuation. Comput. Environ. Urban. Syst. 80. https://doi.org/10.1016/j.compenvurbsys.2019.101452.